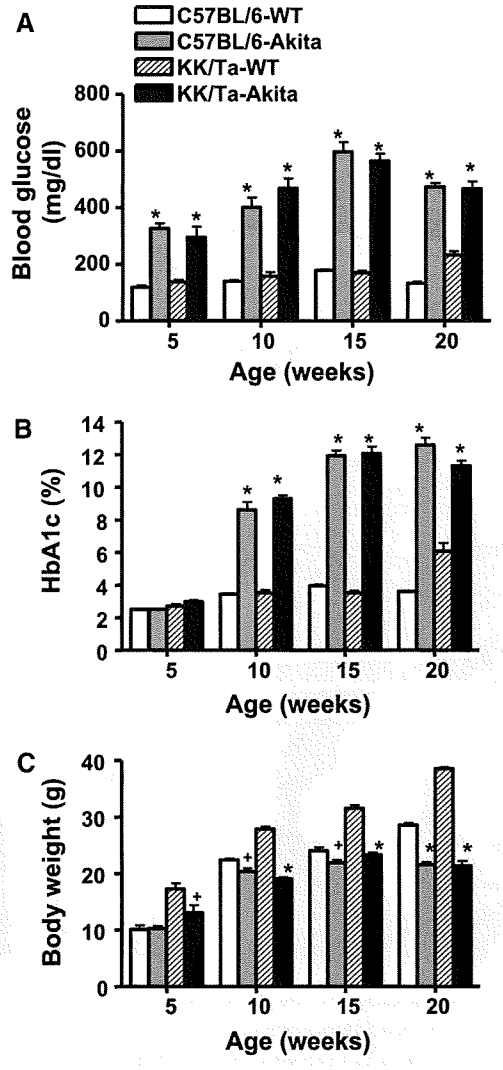

Figure 1. Development of diabetes in male KK/Ta-Akita and C57BL/6-Akita mice. Six hours-fasting blood glucose (A), HbA_{1c} (B), and body weight (C) were measured every 5 wk after birth. Values are means ± SEM of at least eight mice. *$P < 0.001$; +$P < 0.05$ *versus* counterpart WT mice.

albuminuria became pronounced as the mice aged, exceeding 600 of albumin-to-creatinine ratio (ACR), whereas the increase in urine albumin in C57BL/6-Akita males was very small and insignificant even at 20 wk of age (Figure 2A). Mild albuminuria was also observed in KK/Ta-WT males at 20 wk of age. Figure 2B shows GFR in KK/Ta-Akita and C57BL/6-Akita males. Both KK/Ta-Akita and C57BL/6-Akita males exhibited increased GFR at 10 and 15 wk of age as compared with WT mice, indicating development of glomerular hyperfiltration in these mice. Notably, GFR in KK/Ta-Akita males declined at 20 wk of age, whereas reduction of GFR was not observed in C57BL/6-Akita males. Figure 2C shows left kidney weight-to-body weight ratio (LKW/BW) in these mice. KK/Ta-Akita showed significantly increased LKW/BW as early as 5 wk of age as compared with KK/Ta-WT males, and this became more evident at 15 wk of age, demonstrating prominent diabetic renal hypertrophy in KK/Ta-Akita mice (Figure 2C). Statistically, significant increase in LKW/BW was not observed in C57BL/6-Akita males at these time points.

Renal histopathology was assessed by light and electron microscopy. Figure 3A shows representative glomerular light micrographs from KK/Ta-Akita and C57BL/6-Akita males. Moderate mesangial expansion, as evidenced by increased accumulation of periodic acid-Schiff (PAS)-positive material in the mesangial area, was observed in 15-wk-old KK/Ta-Akita males (Figure 3Ad), whereas mesangial expansion was relatively mild in 15-wk-old C57BL/6-Akita males (Figure 3Ab). KK/Ta-WT and C57BL/6-WT mice showed normal glomerular histology. Semiquantitative analysis of PAS-stained kidney sections revealed significantly higher mesangial expansion score in 15-wk-old KK/Ta-Akita males as compared with KK/Ta-WT and C57BL/6-Akita mice (Figure 3C). Glomerular lesions in KK/Ta-Akita males progressed as the mice aged, and prominent mesangial expansion and glomerulosclerosis were observed in approximately 40% of glomeruli at 20 wk of age (Figure 3A, e and f). Arteriolar hyalinosis and focal tubulointerstitial fibrosis were also noted in 20-wk-old KK/Ta-Akita mice (data not shown). Figure 3B shows representative glomerular electron micrographs from the 15-wk-old KK/Ta-Akita mice. Mesangial matrix expansion and irregular thicken-

Table 1. Physiological parameters of C57BL/6-Akita and KK/Ta-Akita mice

Parameter	C57BL/6		KK/Ta	
	WT	Akita	WT	Akita
Systolic blood pressure (mmHg)	93 ± 2	109 ± 6	118 ± 2[b]	126 ± 4[c]
Plasma creatinine (mg/dl)[a]	0.152 ± 0.007	0.178 ± 0.008	0.125 ± 0.004	0.248 ± 0.030[d]
BUN (mg/dl)	27.0 ± 3.6	41.8 ± 2.5	31.1 ± 0.7	45.1 ± 4.2[e]
Total cholesterol (mg/dl)	81.0 ± 4.6	66.2 ± 3.4	83.3 ± 4.2	106.9 ± 15.7[f]
Trigriceride (mg/dl)	63.8 ± 7.3	62.0 ± 4.3	185.3 ± 18.3[b]	192.4 ± 23.1[c]

Values are means ± SEM The data of 15-wk-old mice are shown. $n = 5$ to 8 per group.
[a]The data indicates plasma creatinine levels at 20 wk of age.
[b]$P < 0.01$ *versus* C57BL/6-WT.
[c]$P < 0.01$ *versus* C57BL/6-Akita.
[d]$P < 0.01$ *versus* KK/Ta-WT.
[e]$P < 0.05$ *versus* KK/Ta-WT.
[f]$P < 0.05$ *versus* C57BL/6-Akita.

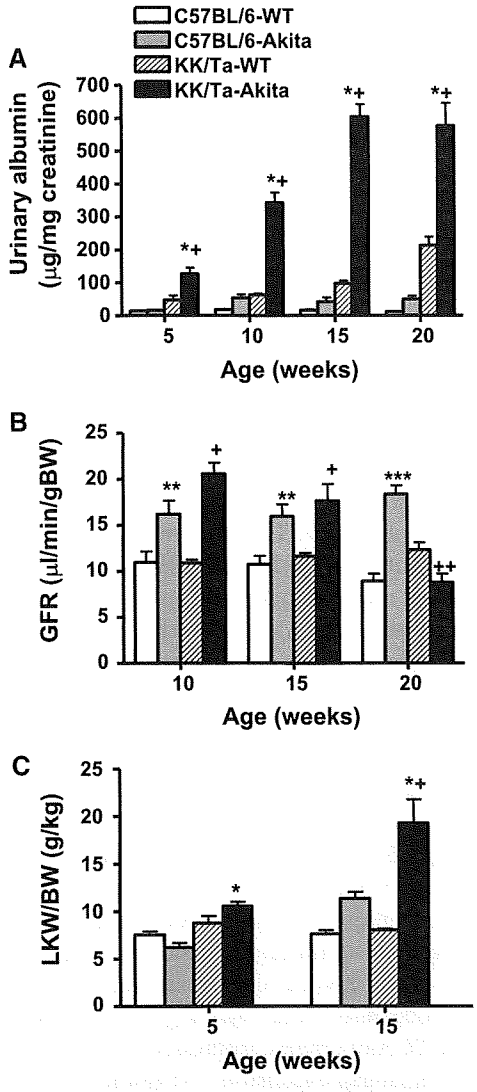

Figure 2. Renal changes in male KK/Ta-Akita and C57BL/6-Akita mice. (A) Urinary albumin excretion was assessed by the determination of urine ACR ($n = 8$ per group). (B) GFR was measured by FITC-inulin clearance method in conscious mice ($n = 8$ per group). (C) LKW/BW was assessed at 5 and 15 wk of age ($n = 6$ per group). Values are means ± SEM. *$P < 0.001$ *versus* C57BL/6-Akita mice; +$P < 0.001$; ++$P < 0.05$ *versus* KK/Ta-WT mice; **$P < 0.05$; ***$P < 0.001$ *versus* C57BL/6-WT mice.

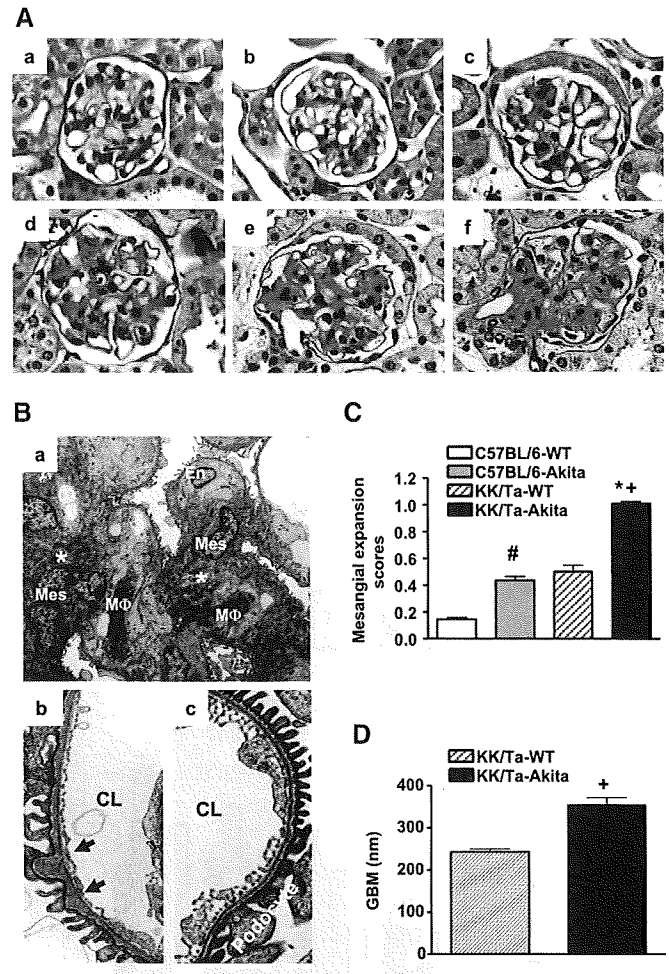

Figure 3. Morphology of KK/Ta-Akita glomeruli. (A) Representative glomerular histopathology in each group mice at 15 to 20 wk of age. (a) C57BL/6-WT (15 wk old), (b) C57BL/6-Akita (15 wk old), (c) KK/Ta-WT (15 wk old), (d) KK/Ta-Akita (15 wk old), (e and f) KK/Ta-Akita (20 wk old). PAS stain, original magnification: ×400. (B) Representative glomerular electron micrographs from 15-wk-old KK/Ta-Akita and KK/Ta-WT mice. (a and b) KK/Ta-Akita, (c) KK/Ta-WT. Arrows indicate irregular thickening of GBM. Asterisks indicate mesangial matrix expansion. CL, capillary lumen; En, endothelial cells; MΦ, macrophage; Mes, mesangial cells. Original magnification, ×5000 in a) ×15,000 in b and c. (C) Glomerular mesangial expansion scores of 15-wk-old mice. The scores were determined on perfusion-fixed PAS-stained kidney sections as described in the Concise Methods section. Data are presented as means ± SEM. #$P < 0.001$ *versus* C57BL/6-WT mice; *$P < 0.001$ versus C57BL/6-Akita mice; +$P < 0.001$ *versus* KK/Ta-WT mice; $n = 6$ per group. (D) GBM thickness in 15-wk-old KK/Ta-Akita and KK/Ta-WT mice. Data are presented as means ± SEM; +$P <$ 0.0001 *versus* KK/Ta-WT mice; $n = 6$ per group.

ing of glomerular basement membrane (GBM) were evident in KK/Ta-Akita mice (Figure 3B, a and b). Morphometric analysis revealed a significant increase in GBM thickness in KK/Ta-Akita males compared with KK/Ta-WT males (Figure 3D). In addition, subendothelial insudation, mesangiolysis, local foot process effacement, and macrophage infiltration were observed in the KK/Ta-Akita glomeruli. No electron dense deposits were observed in the KK/Ta-Akita glomeruli. Obvious ultrastructural changes were not observed in C57BL/6-Akita glomeruli other than mild mesangial matrix accumulation. KK/Ta-WT and C57BL/6-WT mice showed normal glomerular morphology.

Superoxide Production and SOD Activity in KK/Ta-Akita and C57BL/6-Akita Kidneys

To explore the mechanism by which KK/Ta-Akita mice show different susceptibility to DN, next we examined their renal superoxide production, which is thought a central pathogenic pathway in this disease. KK/Ta strain mouse is known to de-

velop obesity (exceeding 35 g of body weight) from 17 to 18 wk of age and become diabetic at around 20 wk of age (phenotypic data; CLEA Japan). Indeed, 20-wk-old KK/Ta-WT males showed higher blood glucose levels, body weight, and urine ACR, than C57BL/6-WT males (Figures 1 and 2). We therefore used 15-wk-old mouse kidneys for this investigation. Renal superoxide levels were assessed by water-soluble tetrazolium salt [2-(4-Iodophenyl)-3-(4-nitrophenyl)-5-(2, 4-disulfophenyl)-2H-tetrazolium; WST-1] method and dihydroethidium (DHE) histochemistry. The specificity of the assay was confirmed by pretreating the samples with polyethylene glycol (PEG)-SOD protein. Consistent with previous reports,[26] superoxide production was increased in the kidneys of C57BL/6-Akita and KK/Ta-Akita mice as compared with nondiabetic mice (Figure 4A). More importantly, the level of superoxide in KK/Ta-Akita kidney was significantly higher than that in C57BL/6-Akita kidney, despite comparable levels of hyperglycemia. Furthermore, glomeruli of KK/Ta-Akita mice showed stronger hydroethidium fluorescence than C57BL/6-Akita glomeruli, indicating increased glomerular superoxide in the mice. With the finding that KK/Ta-WT and C57BL/6-WT mice showed comparable levels of renal superoxide, these data suggested increased superoxide production and/or impaired antioxidant defense capacity in KK/Ta-Akita kidneys. Therefore, we next examined alteration of SOD antioxidant enzyme in KK/Ta-Akita and C57BL/6-Akita kidneys. SOD activity in kidney tissue extracts was determined by inhibition rate of WST-1 reduction reaction.[27] Renal expression of SOD isoform was assessed by western blot analysis. As shown in Figure 4C, SOD activity was significantly reduced in the KK/Ta-Akita kidneys at 15 wk of age as compared with KK/Ta-WT or C57BL/6-Akita kidneys, while there was no difference in renal SOD activity among the four groups at 5 wk of age. Furthermore, Western blot analysis revealed remarkably reduced SOD1 and SOD3 proteins in the 15-wk-old KK/Ta-Akita kidneys, whereas SOD downregulation was not observed in C57BL/6-Akita kidneys (Figure 4D). Reduction of SOD2 protein was not observed in both KK/Ta-Akita and C57BL/6-Akita kidneys (Figure 4D). The downregulation of SOD1 and SOD3 proteins was not observed in 5-wk-old KK/Ta-Akita kidneys (data not shown).

To date, several intracellular pathways were implicated in superoxide overproduction in diabetic vasculature. These include NADPH oxidase, uncoupled eNOS, xanthine oxidase, and mitochondrial respiratory chain enzymes. Among these pathways, NADPH oxidase and uncoupled eNOS were shown to serve as a major source of glomerular superoxide in a diabetic animal.[28] We therefore investigated alteration of these two enzymes in KK/Ta-Akita kidneys (data not shown). However, no difference was observed in renal NADPH oxidase activity between C57BL/6-Akita and KK/Ta-Akita kidneys, yet these kidneys exhibited significantly higher NADPH oxidase activity as compared with nondiabetic counterparts. Furthermore, the eNOS expression was downregulated in KK/Ta-Akita kidneys as compared with C57BL/6-Akita kidneys. Consequently, these findings suggest that the increase in ROS in this model may largely result from the disruption of SOD antioxidant defense system.

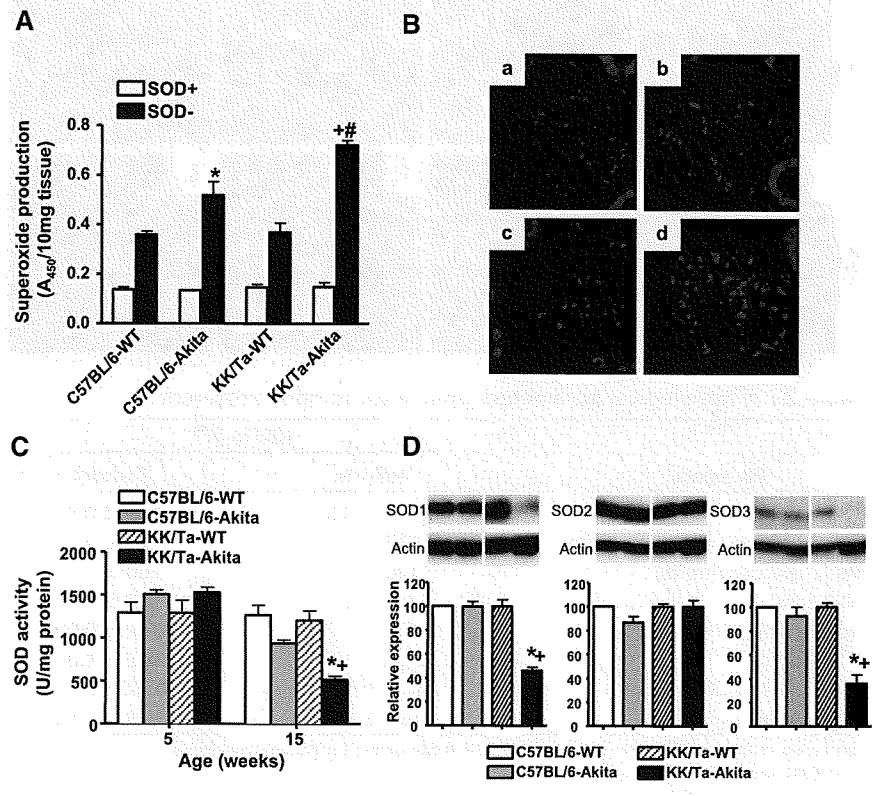

Figure 4. Renal superoxide production and SOD activity and expression in KK/Ta-Akita and C57BL/6-Akita mice. (A) Renal superoxide production in 15-wk-old mice. Data are presented as means ± SEM. SOD+, kidney tissue preincubated with SOD-PEG protein. SOD-, kidney tissue without SOD-PEG protein. *$P < 0.05$ *versus* SOD- C57BL/6-WT kidney; +$P < 0.001$ *versus* SOD- KK/Ta-WT kidney; #$P < 0.01$ *versus* SOD- C57BL/6-Akita kidney; $n = 6$ per group. (B) Representative glomerular DHE staining in 15-wk-old mice. (a) C57BL/6-WT, (b) C57BL/6-Akita, (c) KK/Ta-WT, (d) KK/Ta-Akita. Original magnification, ×400. (C) Renal SOD activity at 5 and 15 wk of age. Data are presented as means ± SEM. *$P < 0.05$ *versus* C57BL/6-Akita mice; +$P < 0.001$ *versus* KK/Ta-WT mice; $n = 8$ per group. (D) Western blot analysis of renal SOD isoform expression in 15-wk-old mice. The relative intensity of SOD-to-actin ratio to the C57BL/6-WT mice is also shown (lower panel). Data are presented as means ± SEM. +$P < 0.001$ *versus* KK/Ta-WT mice; *$P < 0.001$ *versus* C57BL/6-Akita mice; $n = 4$ per group.

Renal Expression of SOD Isoforms in KK/Ta-Akita and C57BL/6-Akita Mice

To determine the cell type responsible for the SOD down-regulation in KK/Ta-Akita kidney, we further investigated the renal SOD isoform expression by immunofluorescence histochemistry. As shown in Figure 5, SOD1 and SOD2 were broadly immunolabeled in multiple renal cell types, including glomerular cells and tubular epithelium. Compared with SOD1, dominant SOD2 immunoreactivity was observed in proximal tubules, and SOD2 was low levels in glomerulus. In contrast, high level of SOD3 expression was observed in glomerular capillary and arterial/arteriolar wall (not shown), and its expression was highly restricted to these sites. There was no difference in the pattern of SOD isoform expression between C57BL/6-WT and KK/Ta-WT kidneys. Consistent with the results of western blot analysis, SOD1 and SOD3 immunoreactivity were reduced in the 15-wk-old KK/Ta-Akita kidney (Figure 5, D and L), whereas their expression were unaltered in C57BL/6-Akita kidney (Figure 5, B and J). SOD1 down-regulation was observed in tubular epithelium as well as in glomerulus in KK/Ta-Akita kidney. SOD2 immunoreactivity was not altered in both C57BL/6-Akita and KK/Ta-Akita kidneys.

Effects of Tempol on DN in KK/Ta-Akita Mice

To determine the significance of SOD downregulation in DN of KK/Ta-Akita mice, we next treated KK/Ta-Akita mice with the membrane-permeable, metal-free SOD mimetic 4-hydroxy-2,2,6,6-tetramethylpiperidine-*N*-oxyl (tempol) and asked whether supplementation of SOD activity ameliorates DN of the KK/Ta-Akita mice. Ten-week-old KK/Ta-Akita and KK/Ta-WT mice were treated either with tempol (1 mmol/L in drinking water) or vehicle for 4 wk ($n = 6$ for each group). Blood parameters, BP, urinary albumin excretion, and GFR were measured before and after 4 wk of tempol treatment. Renal superoxide production and LKW/BW were assessed at the end of treatment. Histologic analysis was performed on PAS-stained kidney sections after 4 wk of treatment. Table 2 shows the physiologic parameters in tempol-treated or vehicle-treated KK/Ta-WT and KK/Ta-Akita mice. Shown in the Table 2, 4-wk tempol treatment did not alter blood glucose, HbA_{1c},

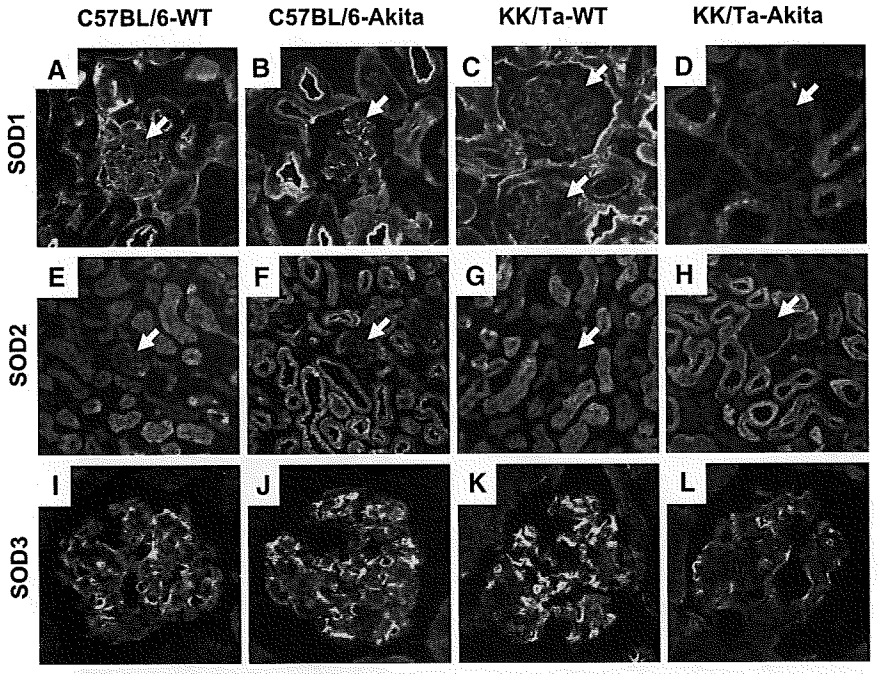

Figure 5. Immunofluorescence SOD isoform staining of 15-wk-old mouse kidney sections. (A to D) SOD1, (E to H) SOD2, (I to L) SOD3, (A, E, and I) C57BL/6-WT mice, (B, F, and J) C57BL/6-Akita mice, (C, G, and K) KK/Ta-WT mice, (D, H, and L) KK/Ta-Akita mice. Arrows indicate glomeruli. Original magnification, ×200 in A through D, ×100 in E through H, and ×400 in I through L.

Table 2. Physiological parameters after 4-wk tempol treatment

Parameter	KK/Ta-WT		KK/Ta-Akita	
	Vehicle	Tempol	Vehicle	Tempol
Body weight (g)	30.1 ± 0.5	31.2 ± 0.9	23.1 ± 0.9	21.6 ± 0.7
Systolic blood pressure (mmHg)	113 ± 4	116 ± 2	122 ± 3	117 ± 5
Blood glucose (mg/dl)	100 ± 19	100 ± 4	519 ± 34	486 ± 29
HbA_{1c} (%)	3.7 ± 0.1	3.7 ± 0.1	12.3 ± 0.4	11.5 ± 0.2
Plasma creatinine (mg/dl)	0.135 ± 0.003	0.149 ± 0.022	0.165 ± 0.014	0.176 ± 0.014
BUN (mg/dl)	23.0 ± 1.4	22.2 ± 1.0	44.1 ± 4.1	42.0 ± 5.8
Total cholesterol (mg/dl)	87.7 ± 6.6	83.7 ± 6.2	147.4 ± 10.4	139.8 ± 15.5
Trigriceride (mg/dl)	202.4 ± 10.5	195.9 ± 12.3	202.8 ± 10.6	112.0 ± 17.9[a]

Values are means ± SEM. $n = 6$ per group; $n = 4$ per group for plasma creatinine.
[a] $P < 0.01$ *versus* KK/Ta-Akita vehicle.

body weight, systolic BP, plasma creatinine, BUN, and total cholesterol levels in KK/Ta-Akita mice. However, the tempol treatment dramatically reduced albuminuria and suppressed elevation of GFR and renal hypertrophy close to the levels of KK/Ta-WT mice (Figure 6, A, B, and C). In agreement with the improvement in renal functions, glomerular DHE stain and renal superoxide levels were significantly reduced in the tempol-treated KK/Ta-Akita mice (Figure 6D). Finally, tempol-treated KK/Ta-Akita mice showed limited mesangial matrix expansion as compared with the vehicle-treated group (Figure 6, E and F). In aggregate, these findings suggest that reduction of renal SOD enzyme may play a key role in the development of overt DN.

DISCUSSION

Our data clearly indicate that two Akita diabetic mouse models, C57BL/6-Akita and KK/Ta-Akita, exhibit differential susceptibility to DN, despite comparable levels of hyperglycemia. KK/Ta-Akita mice develop overt albuminuria as the mice age, whereas C57BL/6-Akita mice are relatively resistant to the development of albuminuria. In addition, the time course of diabetic renal disease in KK/Ta-Akita mice resembles that in human DN. KK/Ta-Akita mice exhibit glomerular hyperfiltration early after the onset of diabetes followed by mesangial expansion, GBM thickness, and a progressive decline in GFR. Although an increase in urine albumin excretion was already observed in KK/Ta-Akita mice at 5 wk of age, this could be because approximately 50% of Akita mice develop hyperglycemia soon after weaning.[23] It is known that KK/Ta mouse strain develops obesity and insulin resistance from 17 to 18 wk of age and becomes diabetic at around 20 wk of age.[25] Therefore, a decline in GFR in KK/Ta-Akita mice at 20 wk of age may be caused by these factors. However, we think this is unlikely as there is no obesity in KK/Ta-Akita mice. Thus, C57BL/6-Akita and KK/Ta-Akita mice provided us a platform for comparative analysis of renal SOD enzyme in the development of overt DN without use of chemicals such as STZ or alloxan, which were documented to generate ROS.[29] Furthermore, the involvement of a single gene, *Ins2*, in the induction of diabetes in this model minimizes a possible involvement of complex traits for DN.

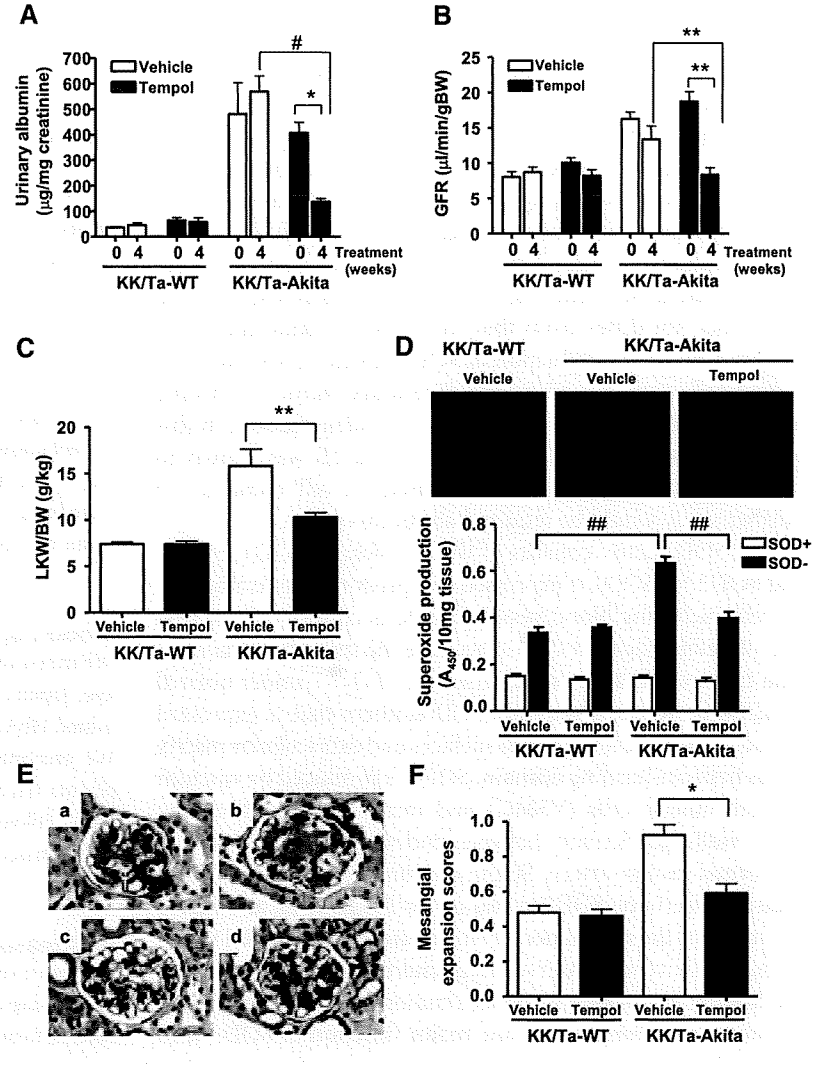

Figure 6. Effects of tempol on DN in KK/Ta-Akita mice. The tempol treatment started at 10 wk of age (0 wk) and ended at 14 wk of age (4 wk). (A) Changes in urinary albumin excretion levels. Values are means ± SEM. $*P < 0.01$; $\#P < 0.0001$; $n = 6$ per group. (B) Changes in GFR. Values are means ± SEM. $**P < 0.05$; $n = 6$ per group. (C) LKW/BW in KK/Ta-WT and KK/Ta-Akita mice after 4-wk treatment. Values are means ± SEM. $**P < 0.05$; $n = 6$ per group. (D) Representative glomerular DHE stain (upper panels) and renal superoxide production (lower panel) in KK/Ta-WT and KK/Ta-Akita mice after 4-wk treatment. Data are presented as means ± SEM. $\#\#P < 0.001$; $n = 5$ per group. SOD+, kidney tissue preincubated with SOD-PEG protein; SOD-, kidney tissue without SOD-PEG protein. Original magnification (upper panels), ×400. (E) Representative light microscopic images of the KK/Ta-Akita glomeruli after 4-wk treatment. (a and b) vehicle-treated, (c and d) tempol-treated. PAS stain, original magnification, ×400. (F) Glomerular mesangial expansion scores in KK/Ta-WT and KK/Ta-Akita mice after 4-wk treatment. Values are means ± SEM. $*P < 0.01$; $n = 6$ per group.

The present study demonstrates that renal SOD activity is reduced in the KK/Ta-Akita mice that develop overt DN, concomitant with remarkable down-regulation of renal SOD1 and SOD3 proteins. Furthermore, DN in KK/Ta-Akita mice was effectively suppressed by SOD mimetic, although severity of diabetes was not altered by the treatment. These findings emerged an important role of renal SOD enzyme in the development of overt DN. It is known that SOD enzyme is up-regulated in response to an increase in oxidative stress.[30,31] This is a critical cellular defense mechanism against excessive oxidative stress. It is therefore conceivable that reduction of SOD enzyme in the diabetic condition causes cytotoxic levels of superoxide overproduction, leading to diabetic renal cell injury. Several studies have investigated renal SOD activity and expression in rodent models of diabetic nephropathy. These include db/db mouse,[19,32] KKAy mouse,[33] and STZ mouse or rat.[33–36] However, these investigations showed up-regulated or unaltered renal SOD activity. With the fact that nephropathy in these rodent models is milder than that in KK/Ta-Akita mice, these findings suggest that SOD downregulation (disruption of an adaptive renal response to increased oxidative stress) may be a key pathogenic mechanism in the progression of DN. It is noteworthy that C57BL/6-Akita mice do not develop overt DN despite of increased renal superoxide levels; the finding suggests that the level of renal SOD activity may be a critical determinant for the development of overt DN.

The decrease in renal SOD activity was not observed in KK/Ta-Akita mice at 5 wk of age, despite the fact that they were already diabetic at this age. Rather, both KK/Ta-Akita and C57BL/6-Akita mice showed higher values of SOD activity than nondiabetic mice. This finding suggests that initial response of renal SOD enzyme to hyperglycemia in KK/Ta-Akita mice does not differ from that in C57BL/6-Akita mice. It is therefore likely that reduction of SOD enzyme in KK/Ta-Akita mouse kidney is caused by the secondary factor of chronic hyperglycemia, such as hypertension or inflammation. In this context, it is of interest that TNFα or IL-1β was shown to down-regulate SOD1 or SOD3 protein in cell cultures.[37,38] Further study would be required about this point.

The SOD family consists of three isoforms, SOD1, SOD2, and SOD3.[8,10] SOD1 is expressed as a predominant isoform in all cells including blood vessels. SOD2 is considered the first line of defense against $O_2^{\bullet -}$, because the mitochondria electron transport chain is a major source of $O_2^{\bullet -}$ under normal conditions. SOD3 is the only SOD isoform that is expressed extracellularly, binding to cell surfaces and extracellular matrix via its heparin-binding domain. SOD3 is produced by vascular smooth muscle cells (VSMC) and localized throughout the vessel walls, particularly between endothelium and VSMC.[39] In normal mouse artery, SOD1 accounts for 50% to 80% of total SOD activity, SOD2 accounts for 2% to 12%, and SOD3 accounts for the remainder.[10,40] Like artery, evident SOD3 immunoreactivity was observed in glomerular microvasculature; the finding implicates SOD3 as a major SOD isoform in glomerulus. It is thought that one major function of SOD3 is to protect nitric oxide (NO) activity as it diffuses from endothelium to VSMC. SOD3$^{-/-}$ mice showed decreased basal NO activity and impaired endothelium-dependent relaxation.[41] SOD3 deficiency was also shown to increase arterial pressure in two models of hypertension.[41,42] Furthermore, gene transfer of SOD3 reduced vascular superoxide levels and increased NO bioactivity in the spontaneously hypertensive rat (SHR).[43] It has been suggested that SOD1 and SOD3 are major determinants of NO bioavailability in blood vessels.[39] Thus, it is conceivable that downregulation of both SOD1 and SOD3 enzymes may largely increase superoxide levels in the glomerular microvasculature and also reduce bioactivity of glomerular NO, resulting in advanced DN. Indeed, an important role of SOD1 in DN was suggested by a recent study demonstrating that the SOD1-deficient mouse exhibits accelerated renal injury with high-dose STZ model.[44] It would be important to determine the precise role of SOD1 and SOD3 enzymes in DN using SOD isoform-deficient spontaneously diabetic mice.

Thus, the present study demonstrates a crucial role of renal SOD enzyme in the development of overt DN. Further efforts to elucidate the molecular mechanism by which chronic hyperglycemia disrupts the renal SOD antioxidant defense system would give a new insight into pathogenesis of DN and lead to better treatment protocol for this disease.

CONCISE METHODS

Animals

C57BL/6 and KK/Ta mice were purchased from CLEA Japan (Tokyo, Japan). *Ins2*^{Akita} mice with C57BL/6 background were from SLC (Hamamatsu, Japan). *Ins2*^{Akita} mice with KK/Ta background were generated by backcrossing male C57BL/6-Akita mice to KK/Ta females for 10 generations. Genotyping was performed as described previously.[22] The mice were allowed unrestricted access to standard rodent chow and water. All animals were treated in accordance with the Animal Welfare Guidelines of Akita University, and all procedures were approved by the Committee on Animal Experimentation of Akita University.

Blood Parameter Measurements

We measured blood glucose using Glucocard Diameter (Arkray, Tokyo, Japan) on samples obtained after a 6-h daytime fast. We determined HbA_{1c} levels using a DCA 2000 Analyzer (Bayer, Elkhart, IN). We enzymatically measured BUN, plasma total cholesterol, and plasma triglycerides by an autoanalyzer (Fuji Dry-Chem 5500; Fuji Film, Tokyo, Japan). We determined plasma creatinine levels by a HPLC-based method as described previously.[45]

BP Measurement

We measured systolic BP in conscious trained mice at room temperature using a noninvasive tail cuff and pulse transducer system (BP-98A; Softron, Tokyo, Japan).

Urine Albumin and Creatinine

We assessed urinary albumin excretion by determination of ACR on morning spot urine as described previously.[21] We measured urine albumin by Albuwell-M Murine Microalbuminuria ELISA kit (Exocell, Philadelphia, PA), and we determined urine creatinine levels using the Creatinine Companion kit (Exocell).

Measurement of GFR

We measured GFR by a single-bolus FITC-inulin injection method as described previously.[46]

Histologic Analysis

We assessed renal histopathology at 15 and 20 wk of age. We anesthetized the mice by an intraperitoneal injection of pentobarbital sodium (50 mg/kg body wt), and we perfused the kidneys with PBS and then with 4% paraformaldehyde in PBS via left ventricle. The kidneys were removed, weighed, and fixed overnight in 4% paraformaldehyde in PBS at 4°C. We stained 2-μm-thick paraffin sections with PAS. We used a semiquantitative score to evaluate the degree and extent of glomerular mesangial expansion as described previously.[21] We analyzed six mice per group and assessed more than 60 glomeruli in each mouse. For electron microscopic examination, we perfused the kidneys with PBS, removed them, cut the cortex into small tissue fragments (1 mm^3), and then fixed them in 3% glutaraldehyde in 0.1 mol/L cacodylate buffer (pH 7.4) overnight at 4°C. The kidney fragments were embedded in Epon resin by standard methods. We observed the sections using a H-7650 transmission electron microscope (Hitachi, Tokyo, Japan) at 80 kV. The thickness of GBM was measured using the H-7650 software (Hitachi). The measurements were undertaken perpendicularly from the endothelial cytoplasmic membrane to the outer lining of the lamina rata externa underneath the cytoplasmic membrane of the epithelial foot process. We assessed at least five glomeruli (total of 75 intercepts) per mouse, and we determined the mean GBM thickness for each mouse. Six mice were analyzed for each group.

Renal Superoxide Production

We assessed the levels of renal superoxide by WST-1 reduction assay and DHE histochemistry as described previously.[27,47] WST-1 is reduced by $O_2^{\bullet -}$ to WST-1 formazan, whose levels can be measured by the absorption at 450 nm. DHE is converted by $O_2^{\bullet -}$ to hydroethidium (Eth), which binds to DNA and produces the Eth-DNA red fluorescence. We used PBS-perfused and freshly removed kidneys for WST-1 reduction assay. We incubated 10 mg kidney cortex tissue with 200 μl WST-1 solution (Dojindo Molecular Technologies, Gaithersburg, MD) for 1 h at 37°C. After centrifugation at 10,000 × *g* for 10 min, we transferred the supernatant (150 μl for each sample) to a 96-well microplate and measured the absorbance at 450 nm. The specificity of the assay was confirmed by preincubating the kidney tissue with SOD-PEG (20 U; Sigma-Aldrich, St. Louis, MO) overnight at 37°C. For DHE staining, kidneys were perfusion-fixed with 4% paraformaldehyde, and the tissues were immersed in 20% sucrose in PBS and frozen with OCT compound (Sakura Finetechnical Co., Tokyo, Japan). We incubated cryostat sections with 200 μmol/L DHE (Sigma-Aldrich) for 1 h at 37°C, and we examined the Eth-DNA fluorescence at 480-nm excitation and 610-nm emission using a LSM510 confocal laser-scanning microscope (Carl Zeiss, Oberkochen, Germany).

Renal SOD Activity

We determined SOD activity in whole kidney tissue lysate using a SOD assay kit-WST (Dojindo Molecular Technologies) as described previously.[27] We measured the amount of protein using a bicinochoninic acid protein assay (Sigma-Aldrich). Enzymatic activity was expressed in units per mg protein.

Western Blot Analysis

PBS-perfused kidney cortex tissues were homogenized in lysis buffer (0.25 M sucrose, 10 mM Tris, 1 mM EDTA, pH 7.4), centrifuged at 10,000 × g for 10 min at 4°C, and the cleared lysate was used for western blot analysis. We determined the amount of protein using a bicinochoninic acid protein assay. Twenty micrograms protein were separated by SDS-PAGE, and transferred onto polyvinylidene difluoride membranes (Bio-Rad Laboratories, Hercules, CA). After blocking, the membranes were reacted with: (i) rabbit anti-Cu/Zn SOD (SOD1) (1:10,000; Stressgen, Ann Arbor, MI); (ii) rabbit anti-Mn SOD (SOD2) (1:10,000; Stressgen); and (iii) rabbit anti-EC SOD (SOD3) (1:2000; Stressgen) polyclonal antibodies. After washing, we incubated the membranes with HRP-conjugated goat anti-rabbit IgG antibody (1:10,000; DakoCytomation, Glostrup, Denmark). We visualized the reactions using an enhanced chemiluminescence (ECL) detection system (Amersham Pharmacia Biotech, Buckinghamshire, UK). Loading of lysate protein was evaluated by immunoblot using rabbit anti-actin antibody (1:1000; Sigma-Aldrich) and HRP-conjugated goat anti-rabbit IgG antibody (DakoCytomation). The intensity of the signals was semiquantified using Adobe Photoshop (version 5.5; Adobe Systems, San Jose, CA) and determined by subtracting background of the adjacent area.

Immunohistochemistry

Cryostat sections were prepared as described in DHE histochemistry. We blocked the sections and labeled them with rabbit anti-Cu/Zn SOD (SOD1) (1:100; Stressgen), rabbit anti-Mn SOD (SOD2) (1:100; Stressgen), or rabbit anti-EC SOD (SOD3) (1:50; Stressgen) polyclonal antibodies for 1 h at room temperature, followed by Alexa Fluor 488-conjugated goat anti-rabbit IgG antibody (1:200; Molecular Probes, Eugene, OR) for 30 min at room temperature. We then counterstained the sections with ToPro-3 (Molecular Probes) and took images using the LSM510 confocal laser-scanning microscope.

Treatment with Tempol

Metal-free SOD mimetic tempol (Sigma-Aldrich) was added in the drinking water (1 mmol/L) and given to the mice *ad libitum* for 4 wk as described previously.[44,48] Control group mice were given the same water alone as vehicle.

Statistical Analysis

We presented all data as means ± SEM. We performed statistical analysis of the data using GraphPad Prism software (GraphPad, San Diego, CA). For comparisons between two groups, we used an un-

paired t test to assess statistical significance. We determined differences between multiple groups by one-way ANOVA followed by Bonferroni multiple comparison test. $P < 0.05$ was considered statistically significant.

ACKNOWLEDGMENTS

This work was supported by a Grant-in-Aid for Scientific Research (no. 20590943 to H.F.) from the Ministry of Education, Science, and Culture, Japan, and National Institutes of Health grants (DK39261 to T.T. and R.C.H., and DK61018 to M.D.B.). We thank Ms. Kayoko Kagaya (Akita University School of Medicine) for technical assistance and Drs. Takuji Shirasawa and Takahiko Shimizu (Tokyo Metropolitan Institute of Gerontology) for suggestions and support. This study was facilitated by the Vanderbilt Mouse Metabolic Phenotyping Center.

DISCLOSURES

None

REFERENCES

1. Krolewski AS: Genetics of diabetic nephropathy: Evidence for major and minor gene effects. *Kidney Int* 55: 1582–1596, 1999
2. Freedman BI, Bostrom M, Daeihagh P, Bowden DW: Genetic factors in diabetic nephropathy. *Clin J Am Soc Nephrol* 2: 1306–1316, 2007
3. Brownlee M: The pathobiology of diabetic complications: A unifying mechanism. *Diabetes* 54: 1615–1625, 2005
4. Brownlee M: Biochemistry and molecular cell biology of diabetic complications. *Nature* 414: 813–820, 2001
5. Li JM, Shah AM: Endothelial cell superoxide generation: regulation and relevance for cardiovascular pathophysiology. *Am J Physiol Regul Integr Comp Physiol* 287: R1014–R1030, 2004
6. Evans JL, Goldfine ID, Maddux BA, Grodsky GM: Oxidative stress and stress-activated signaling pathways: A unifying hypothesis of type 2 diabetes. *Endocr Rev* 23: 599–622, 2002
7. Fridovich I: Superoxide radical and superoxide dismutases. *Annu Rev Biochem* 64: 97–112, 1995
8. Fridovich I: Superoxide anion radical (O2-.), superoxide dismutases, and related matters. *J Biol Chem* 272: 18515–18517, 1997
9. Halliwell B: Antioxidant characterization. Methodology and mechanism. *Biochem Pharmacol* 49: 1341–1348, 1995
10. Faraci FM, Didion SP: Vascular protection: superoxide dismutase isoforms in the vessel wall. *Arterioscler Thromb Vasc Biol* 24: 1367–1373, 2004
11. Hodgkinson AD, Bartlett T, Oates PJ, Millward BA, Demaine AG: The response of antioxidant genes to hyperglycemia is abnormal in patients with type 1 diabetes and diabetic nephropathy. *Diabetes* 52: 846–851, 2003
12. Kedziora-Kornatowska KZ, Luciak M, Blaszczyk J, Pawlak W: Lipid peroxidation and activities of antioxidant enzymes in erythrocytes of patients with non-insulin dependent diabetes with or without diabetic nephropathy. *Nephrol Dial Transplant* 13: 2829–2832, 1998
13. Bhatia S, Shukla R, Venkata Madhu S, Kaur Gambhir J, Madhava Prabhu K: Antioxidant status, lipid peroxidation and nitric oxide end products in patients of type 2 diabetes mellitus with nephropathy. *Clin Biochem* 36: 557–562, 2003
14. Colak E, Majkic-Singh N, Stankovic S, Sreckovic-Dimitrijevic V, Djordjevic PB, Lalic K, Lalic N: Parameters of antioxidative defense in type 2 diabetic patients with cardiovascular complications. *Ann Med* 37: 613–620, 2005
15. Möllsten A, Marklund SL, Wessman M, Svensson M, Forsblom C, Parkkonen M, Brismar K, Groop PH, Dahlquist G: A functional polymorphism in the manganese superoxide dismutase gene and diabetic nephropathy. *Diabetes* 56: 265–269, 2007
16. Lee SJ, Choi MG, Kim DS, Kim TW: Manganese superoxide dismutase gene polymorphism (V16A) is associated with stages of albuminuria in Korean type 2 diabetic patients. *Metabolism* 55: 1–7, 2006
17. Al-Kateb H, Boright AP, Mirea L, Xie X, Sutradhar R, Mowjoodi A, Bharaj B, Liu M, Bucksa JM, Arends VL, Steffes MW, Cleary PA, Sun W, Lachin JM, Thorner PS, Ho M, McKnight AJ, Maxwell AP, Savage DA, Kidd KK, Kidd JR, Speed WC, Orchard TJ, Miller RG, Sun L, Bull SB, Paterson AD; Diabetes Control and Complications Trial/Epidemiology of Diabetes Interventions and Complications Research Group: Multiple superoxide dismutase 1/splicing factor serine alanine 15 variants are associated with the development and progression of diabetic nephropathy: the Diabetes Control and Complications Trial/Epidemiology of Diabetes Interventions and Complications Genetics study. *Diabetes* 57: 218–228, 2008
18. Craven PA, Phillips SL, Melhem MF, Liachenko J, DeRubertis FR: Overexpression of manganese superoxide dismutase suppresses increases in collagen accumulation induced by culture of mesangial cells in high-media glucose. *Metabolism* 50: 1043–1048, 2001
19. DeRubertis FR, Craven PA, Melhem MF, Salah EM: Attenuation of renal injury in db/db mice overexpressing superoxide dismutase: Evidence for reduced superoxide-nitric oxide interaction. *Diabetes* 53: 762–768, 2004
20. Breyer MD, Tchekneva E, Qi Z, Takahashi T, Fogo AB, Zhao HJ, Harris RC: Genetics of diabetic nephropathy: Lessons from mice. *Semin Nephrol* 27: 237–247, 2007
21. Qi Z, Fujita H, Jin J, Davis LS, Wang Y, Fogo AB, Breyer MD: Characterization of susceptibility of inbred mouse strains to diabetic nephropathy. *Diabetes* 54: 2628–2637, 2005
22. Wang J, Takeuchi T, Tanaka S, Kubo SK, Kayo T, Lu D, Takata K, Koizumi A, Izumi T: A mutation in the insulin 2 gene induces diabetes with severe pancreatic beta-cell dysfunction in the Mody mouse. *J Clin Invest* 103: 27–37, 1999
23. Yoshioka M, Kayo T, Ikeda T, Koizumi A: A novel locus, Mody4, distal to D7Mit189 on chromosome 7 determines early-onset NIDDM in nonobese C57BL/6 (Akita) mutant mice. *Diabetes* 46: 887–894, 1997
24. Fujita H, Haseyama T, Kayo T, Nozaki J, Wada Y, Ito S, Koizumi A: Increased expression of glutathione S-transferase in renal proximal tubules in the early stages of diabetes: a study of type-2 diabetes in the Akita mouse model. *Exp Nephrol* 9: 380–386, 2001
25. Tomino Y, Tanimoto M, Shike T, Shiina K, Fan Q, Liao J, Gohda T, Makita Y, Funabiki K: Pathogenesis and treatment of type 2 diabetic nephropathy: Lessons from the spontaneous KK/Ta mouse model. *Curr Diabetes Rev* 1: 281–286, 2005
26. Forbes JM, Coughlan MT, Cooper ME: Oxidative stress as a major culprit in kidney disease in diabetes. *Diabetes* 57: 1446–1454, 2008
27. Ikegami T, Suzuki Y, Shimizu T, Isono K, Koseki H, Shirasawa T: Model mice for tissue-specific deletion of the manganese superoxide dismutase (MnSOD) gene. *Biochem Biophys Res Commun* 296: 729–736, 2002
28. Satoh M, Fujimoto S, Haruna Y, Arakawa S, Horike H, Komai N, Sasaki T, Tsujioka K, Makino H, Kashihara N: NAD(P)H oxidase and uncoupled nitric oxide synthase are major sources of glomerular superoxide in rats with experimental diabetic nephropathy. *Am J Physiol Renal Physiol* 288: F1144–1152, 2005
29. Szkudelski T: The mechanism of alloxan and streptozotocin action in B cells of the rat pancreas. *Physiol Res* 50: 537–546, 2001
30. Chang MS, Yoo HY, Rho HM: Transcriptional regulation and environmental induction of gene encoding copper- and zinc-containing superoxide dismutase. *Methods Enzymol* 349: 293–305, 2002

31. Yoo HY, Chang MS, Rho HM: The activation of the rat copper/zinc superoxide dismutase gene by hydrogen peroxide through the hydrogen peroxide-responsive element and by paraquat and heat shock through the same heat shock element. *J Biol Chem* 274: 23887–23892, 1999
32. Barati MT, Merchant ML, Kain AB, Jevans AW, McLeish KR, Klein JB: Proteomic analysis defines altered cellular redox pathways and advanced glycation end-product metabolism in glomeruli of db/db diabetic mice. *Am J Physiol Renal Physiol* 293: F1157–F1165, 2007
33. Fujita A, Sasaki H, Ogawa K, Okamoto K, Matsuno S, Matsumoto E, Furuta H, Nishi M, Nakao T, Tsuno T, Taniguchi H, Nanjo K: Increased gene expression of antioxidant enzymes in KKAy diabetic mice but not in STZ diabetic mice. *Diabetes Res Clin Pract* 69: 113–119, 2005
34. Kakkar R, Mantha SV, Radhi J, Prasad K, Kalra J: Antioxidant defense system in diabetic kidney: A time course study. *Life Sci* 60: 667–679, 1997
35. Limaye PV, Raghuram N, Sivakami S: Oxidative stress and gene expression of antioxidant enzymes in the renal cortex of streptozotocin-induced diabetic rats. *Mol Cell Biochem* 243: 147–152, 2003
36. Oktem F, Ozguner F, Yilmaz HR, Uz E, Dundar B: Melatonin reduces urinary excretion of N-acetyl-beta-D-glucosaminidase, albumin, and renal oxidative markers in diabetic rats. *Clin Exp Pharmacol Physiol* 33: 95–101, 2006
37. Afonso V, Santos G, Collin P, Khatib AM, Mitrovic DR, Lomri N, Leitman DC, Lomri A: Tumor necrosis factor-alpha down-regulates human Cu/Zn superoxide dismutase 1 promoter via JNK/AP-1 signaling pathway. *Free Radic Biol Med* 41: 709–721, 2006
38. Olofsson EM, Marklund SL, Pedrosa-Domellof F, Behndig A: Interleukin-1alpha downregulates extracellular-superoxide dismutase in human corneal keratoconus stromal cells. *Mol Vis* 13: 1285–1290, 2007
39. Fukai T, Folz RJ, Landmesser U, Harrison DG: Extracellular superoxide dismutase and cardiovascular disease. *Cardiovasc Res* 55: 239–249, 2002
40. Fukai T, Galis ZS, Meng XP, Parthasarathy S, Harrison DG: Vascular expression of extracellular superoxide dismutase in atherosclerosis. *J Clin Invest* 101: 2101–2111, 1998
41. Jung O, Marklund SL, Geiger H, Pedrazzini T, Busse R, Brandes RP: Extracellular superoxide dismutase is a major determinant of nitric oxide bioavailability: *In vivo* and *ex vivo* evidence from ecSOD-deficient mice. *Circ Res* 93: 622–629, 2003
42. Jonsson LM, Rees DD, Edlund T, Marklund SL: Nitric oxide and blood pressure in mice lacking extracellular-superoxide dismutase. *Free Radic Res* 36: 755–758, 2002
43. Fennell JP, Brosnan MJ, Frater AJ, Hamilton CA, Alexander MY, Nicklin SA, Heistad DD, Baker AH, Dominiczak AF: Adenovirus-mediated overexpression of extracellular superoxide dismutase improves endothelial dysfunction in a rat model of hypertension. *Gene Ther* 9: 110–117, 2002
44. DeRubertis FR, Craven PA, Melhem MF: Acceleration of diabetic renal injury in the superoxide dismutase knockout mouse: Effects of tempol. *Metabolism* 56: 1256–1264, 2007
45. Dunn SR, Qi Z, Bottinger EP, Breyer MD, Sharma K: Utility of endogenous creatinine clearance as a measure of renal function in mice. *Kidney Int* 65: 1959–1967, 2004
46. Qi Z, Whitt I, Mehta A, Jin J, Zhao M, Harris RC, Fogo AB, Breyer MD: Serial determination of glomerular filtration rate in conscious mice using FITC-inulin clearance. *Am J Physiol Renal Physiol* 286: F590–F596, 2004
47. Nakamura K, Yamagishi S, Matsui T, Yoshida T, Takenaka K, Jinnouchi Y, Yoshida Y, Ueda S, Adachi H, Imaizumi T: Pigment epithelium-derived factor inhibits neointimal hyperplasia after vascular injury by blocking NADPH oxidase-mediated reactive oxygen species generation. *Am J Pathol* 170: 2159–2170, 2007
48. Schnackenberg CG, Wilcox CS: Two-week administration of tempol attenuates both hypertension and renal excretion of 8-Iso prostaglandin f2alpha. *Hypertension* 33: 424–428, 1999

Diurnal Changes in Urinary Excretion of IgG, Transferrin, and Ceruloplasmin Depend on Diurnal Changes in Systemic Blood Pressure in Normotensive, Normoalbuminuric Type 2 Diabetic Patients

Authors
M. Hosoba[1], H. Fujita[1], T. Miura[1], T. Morii[1], T. Shimotomai[1], J. Koshimura[1], Y. Yamada[1], S. Ito[2], T. Narita[1]

Affiliations
[1] Department of Endocrinology, Diabetes and Geriatric Medicine, Akita University School of Medicine, Akita, Japan
[2] Division of Cardiology, Hematology & Endocrinology/Metabolism, Niigata University Graduate School of Medicine & Dental Science, Niigata, Japan

Key words
- ambulatory blood pressure
- diabetic nephropathy
- microalbuminuria

Abstract

Previous studies of diabetic patients indicate that increased urinary excretion of certain plasma proteins (molecular radii <55 A), such as IgG, transferrin, and ceruloplasmin, precede the development of microalbuminuria. Moreover, increases in these urinary proteins predict future development of microalbuminuria. To clarify whether blood pressure changes influence urinary excretion of these proteins, we examined relationships between diurnal blood pressure changes measured by ambulatory blood pressure monitoring and urinary excretion of IgG, transferrin, ceruloplasmin, α2-macroglobulin (88 A) and albumin (36 A) measured separately during the day and night in 20 healthy controls and 26 normotensive, normoalbuminuric diabetic patients. Diurnal change in systolic blood pressure was not correlated to urinary excretion of either albumin or α2-macroglobulin in either diabetic patients or controls. However, statistically significant correlations between diurnal changes in systolic blood pressure and those of urinary excretion of IgG, transferrin and ceruloplasmin were found in diabetic patients but not in controls. The present findings suggest that urinary excretion of IgG, transferrin, and ceruloplasmin are more easily affected than albuminuria by systemic blood pressure changes in normoalbuminuric diabetic patients. This is supported by our previous finding that urinary excretion of IgG, transferrin and ceruloplasmin increased while albuminuria did not following enhanced glomerular filtration rate after acute protein loading, which causes increased glomerular capillary pressure due to afferent arterioles dilation, mimicking diabetic intra-renal hemodynamics. Taken together, these findings suggest that urinary excretion of IgG, transferrin, and ceruloplasmin may be more sensitive indicators of glomerular capillary pressure change than albuminuria in normoalbuminuric diabetic patients.

received 15.09.2008
accepted after second revision 22.06.2009

Bibliography
DOI 10.1055/s-0029-1233458
Published online: August 7, 2009
Horm Metab Res 2009; 41: 910–915

ISSN 0018-5043

Correspondence
M. Hosoba, MD
Department of Endocrinology Diabetes and Geriatric Medicine
Akita University School of Medicine
Hondo
010-8543 Akita
Japan
Tel.: +81/18/884 60 40
Fax: +81/18/884 64 49
hosoba@med.akita-u.ac.jp

Introduction

Diabetic nephropathy (DN) is the leading cause of end-stage renal disease, not only in the Western world but also in Asian and African populations [1]. Early recognition of renal changes reduces the risk of DN. Microalbuminuria (MA) is generally considered the best available noninvasive predictor of DN. However, several studies including our own have shown that increased urinary excretion of certain plasma proteins with different molecular radii (MR) <55 A and different isoelectric points (pIs), such as IgG [2,3], transferrin (Tf) [4,5], and ceruloplasmin (CRL) [3,6] (MRs are 55 A, 38 A and 45 A; molecular weight [MW] are 155 kDa, 77 kDa and 132 kDa; the pIs are 7.4, 5.7 and 4.4, respectively), except for albumin (Alb; MR, 36 A; MW, 67 kDa; pIs, 4.7) (hereafter collectively abbreviated to small-sized plasma proteins: SPPs), precede the development of MA in diabetic patients. Furthermore, follow-up studies of type 2 diabetic patients, including a study by the present authors, indicate that increased urinary excretion of these proteins at baseline predicts future development of MA [5,7]. The mechanisms of earlier increases in these SPPs in normoalbuminuric diabetic patients remain to be elucidated.

In experimental studies, elevated glomerular capillary pressure (GCP) has been considered one of the principal causes of initiation and progression of DN [8]. Increased GCP in the diabetic state is mainly explained by decreased afferent arteriolar resistance and/or increased efferent arteriolar resistance [8–10]. Given these intra-renal hemodynamic changes, it is assumed that slight eleva-

tion of systemic blood pressure (BP) may easily transmit to the glomerular capillaries in the diabetic kidney, causing glomerular hypertension.

Increased dietary intake of protein elevates glomerular filtration rate (GFR) through dilatation of afferent arterioles and elevation of GCP [11,12], mimicking diabetic intra-renal hemodynamic changes. Recently, we found that urinary excretion of SPPs were selectively increased, in spite of no increased urinary excretion of Alb, when GFR was increased by acute protein loading (APL) in healthy participants [13,14]. In this study, increased urinary excretion of α2-macroglobulin (A2), which has a large MR of 88A (MW, 770kDa; pIs, 5.4), was not detected. Taking these findings together, it is suggested that changes in renal hemodynamics can be predicted by the measurement of urinary excretions of SPPs.

On the basis of these findings, it is assumed that changes in systemic BP would cause changes in urinary excretion of SPPs in diabetic patients through the tendency for GCP lability due to afferent arteriole dilation following systemic BP changes. However, it has not been comprehensively examined whether changes in systemic BP relate to changes in urinary SPPs in normoalbuminuric diabetic patients. The exception is our recent pilot study with small numbers of normoalbuminuric diabetic patients (n=11); this showed that low-dose losartan reversibly decreased urinary excretion of SPPs without changes in albuminuria or urinary A2 excretion and that systemic BP change induced by low-dose losartan correlated with changes in urinary SPP excretion [15]. Therefore, the present study examined relationships between diurnal BP changes and diurnal changes in urinary SPPs using ambulatory BP monitoring (ABPM) in normoalbuminuric diabetic patients.

Participants and Methods

Participants

Twenty-six type 2 diabetic patients (Group A; 19 men and 7 women; age range 30–68 years; mean±SD, 52.2±8.7 years) were recruited to participate in this study from patients who were admitted to our hospital for glycemic control. They fulfilled the following criteria: normoalbuminuria with albumin to creatinine (Cr) ratio of less than 30mg/g Cr on two consecutive spot urine samples; absence of hematuria; and no serological evidence of nondiabetic renal disease. Patients with acute or chronic infections, malignancy, congestive heart failure or nephrolithiasis were excluded from this study. Healthy controls consisted of 9 men and 11 women (Group B; age range 47–58 years, mean±SD, 52.0±3.0 years). Controls were free from renal disease, heart disease, cerebrovascular disease and hypertension. They were normoglycemic and normoalbuminuric, and urinalysis revealed no erythrocytes or other indications of renal diseases. No participants were treated with antihypertensive agents. No controls were treated with antihyperlipidemic agents or with diet therapy prior to this study. On the other hand, four diabetic patients were treated with antihyperlipidemic agents. All participants in this study gave informed consent. The protocol was approved by the Ethics Committee of Akita University School of Medicine (approval number 211).

Study protocol

After admission to our hospital, the patients in Group A were treated with a standard diabetic diet recommended by Japan Diabetes Society [16], which contained approximately 30kcal/kg ideal body weight (BW) and with either antidiabetic drugs (n=8) or insulin (n=17). Ideal BW (kg) was calculated from ideal body mass index as (height [m]^2×22). All diabetic patients were treated with above mentioned diet therapy in the hospital for two weeks prior to this study. Ambulatory blood pressure monitoring (ABPM) was performed for 24h with ABPM FB-250 equipment (Fukuda Denshi, Co. Ltd, Tokyo, Japan), which can measure systolic BP (SBP), diastolic BP (DBP), and heart rate (HR) by the Korotokoff and oscillometric methods, respectively. Measurements were taken every 30min during the day (07:00–21:00h) and every 60min during the night (21:00–7:00h). Participants were instructed to rest or sleep between 21:00–7:00h and to maintain their usual activities between 7:00–21:00h, avoiding heavy physical exercise and alcohol consumption. Daytime and nighttime means and diurnal index (DI, %, calculated as [nighttime mean-daytime mean]/daytime mean]×100) were calculated separately for SBP and DBP. A patient was considered a "nondipper" if his or her nighttime reduction of SBP and DBP (the diurnal index) was less than 10%.

As it is reported that animal or fish protein in the diet causes enhanced GFR followed by increased urinary excretions of SPPs [13,14,17], dietary protein in the present study was limited to cooked vegetable proteins, which have been reported not to affect GFR or urinary excretion of Alb [18,19] or IgG [19]. On the day of ABPM measurement, Group A patients ate a diet prepared by dieticians of our hospital to give a total energy intake of 30kcal/kg BW/day and to contain approximately 1.2g/kg ideal BW/day of protein (this was exclusively vegetable protein). Group B also consumed diets prepared by dieticians to give a total energy intake of 1800kcal/day including 60g/day (equal to approximately 1.2g/kg BW/day) of vegetable proteins. All patients were prohibited from taking foods or beverages other than these prepared diets with the exception of tap water.

Urine samples were collected separately between 7:00–21:00h, and between 21:00–7:00h. Urinary concentrations of IgG, CRL, and A2 were measured by immunoradiometric assay in our laboratory according to procedures previously reported [3,6,13,20]. Levels of Alb and Tf were measured by radioimmunoassay using the double antibody technique [13,14]. The results were expressed as protein-to-creatinine ratios (U-Alb/Cr, U-IgG/Cr, U-Tf/Cr, U-CRL/Cr and U-A2/Cr). For the evaluations of diurnal variations of the urinary excretion of these proteins, DIs of these urinary protein excretion were calculated by the same equation used in the evaluation of DIs of BP. Urinary concentration of Cr, plasma glucose levels and serum concentrations of Cr, total cholesterol, triglycerides and HDL-cholesterol were measured by enzymatic methods using an automated multianalyzer (7600 Hitachi, Tokyo, Japan). HbA1c was measured by high performance liquid chromatography using an automated analyzer (HLC-723GHb V A1c 2.2; Tosoh, Tokyo, Japan). The reference range of HbA1c at our hospital was 4.3–5.8%. All urine and serum samples from the participants were stored at −80°C until required.

Statistical analysis

Values are expressed as means±SD. Mann-Whitney's U test, unpaired Student's *t*-test and χ^2 test were used to calculate whether differences between Groups A and B were statistically significant. Pearson's correlation analysis was performed between DIs of the results of ABPM and those of urinary excretion of Alb, A2, and SPPs. All calculations were performed using

Table 1 Clinical characteristics of 20 healthy controls and 26 normoalbuminuric type 2 diabetic patients

	Controls	Diabetic patients
Number of patients (male/female)	20 (9/11)	26 (19/7)
Age (years)	52.0±3.0	52.2±8.7
Diabetes duration (years)	–	8.8±8.0
BMI (kg/m^2)	22.3±2.6	22.7±3.8
Diabetic retinopathy (nil/simple/proliferative)	–	14/7/5
Antidiabetic treatment (diet/drugs/insulin)	–	1/8/17
Fasting plasma glucose (mmol/l)	5.5±0.4	7.8±1.5*
HbA1c (%)	5.0±0.3	9.9±2.2*
Daytime SBP (mmHg)	119.8±9.7	111.6±14.7¶
Nighttime SBP (mmHg)	100.8±13.9	103.3±14.3
Daytime DBP (mmHg)	78.9±7.1	71.9±7.1**
Nighttime DBP (mmHg)	68.5±9.0	66.5±5.8
dipper/nondipper	17/3	9/17#
Total cholesterol (mmol/l)	5.3±0.6	4.5±0.9**
Triglycerides (mmol/l)	1.0±0.6	1.3±0.9
DI of SBP (%)	−16.1±7.1	−7.0±9.8**
DI of DBP (%)	−13.2±7.5	−7.1±7.5¶
DI of U-IgG/Cr (%)	−42.1±15.4	−22.8±19.6§
DI of U-Tf/Cr (%)	−45.9±32.5	−30.0±23.0¶
DI of U-CRL/Cr (%)	−50.9±23.9	−23.8±25.0**
DI of U-Alb/Cr (%)	−27.0±24.9	−19.5±19.0
DI of U-A2/Cr (%)	14.0±38.6	14.9±26.2

Data are expressed as mean±SD unless otherwise indicated. *p<0.0001 vs. control subjects; §p<0.0005 vs. control subjects; **p<0.005 vs. control subjects; ¶p<0.05 vs. control subjects revealed by Mann-Whitney's U test. #p<0.001 vs. control subjects revealed by χ^2test. U-IgG/Cr, U-Tf/Cr, U-CRL/Cr, U-Alb/Cr and U-A2/Cr represent ratios of urinary immunoglobulin G, transferrin, ceruloplasmin, albumin, and α2 macroglobulin to urinary creatinine in daytime and nighttime urine samples, respectively. DI: diurnal index (% of [nighttime mean-daytime mean]/daytime mean)

the StatView software package (Abacus Concept, Inc, Berkeley, CA, USA).

Results

The clinical characteristics of controls and normoalbuminuric diabetic patients are shown in **Tables 1, 2**. Compared with controls, patients with diabetes had significantly elevated fasting blood glucose and HbA1c levels. Total cholesterol levels were significantly higher in controls than in diabetic patients. Our diabetic patients were treated with antihyperlipidemic agents and all diabetic patients were treated with diet therapy in the hospital for two weeks prior to this study. These conditions may be related with the results that diabetic patients have better total cholesterol than controls.

Although the gender distribution between the diabetic group and control group seems to be uneven, the difference was not statistically significant by χ^2 test.

The proportion of nondippers was significantly higher in diabetic patients than in controls (61.5% vs. 15%, p<0.001). Although there was no difference between controls and diabetic patients for nighttime SBP and DBP, daytime SBP and DBP were higher (still within the normal range) in controls than in diabetic patients. DIs of SBP and DBP were significantly smaller absolute values in diabetic patients than in controls (**Table 1**).

Daytime and nighttime U-Alb/Cr, U-IgG/Cr, U-Tf/Cr, U-CRL/Cr and U-A2/Cr are listed in **Table 2**. The normality analysis of these

Table 2 Urinary excretion of five plasma proteins in daytime and nighttime urine samples in 20 healthy controls and 26 normoalbuminuric type 2 diabetic patients

	Controls		Diabetic patients	
	Daytime	Nighttime	Daytime	Nighttime
U-IgG/Cr (mg/gCr)	3.3±1.1	1.9±0.7	4.3±2.4	3.2±1.9††
U-Tf/Cr (mg/gCr)	0.37±0.16	0.19±0.11	0.57±0.56	0.38±0.38*
U-CRL/Cr (μg/gCr)	62±37	27±13	67±51	47±36*
U-Alb/Cr (mg/gCr)	7.8±3.3	5.3±2.0	13±10*	9.8±6.6††
U-A2/Cr (μg/gCr)	19±33	12±13	33±92	22±47

Data are expressed as mean±SD. ††p<0.01 vs. control subjects; revealed by Mann-Whitney's U test. *p<0.05 vs. control subjects revealed by Student's *t*-test (Mann-Whitney's U test revealed no statistically significance). U-IgG/Cr, U-Tf/Cr, U-CRL/Cr, U-Alb/Cr and U-A2/Cr represent ratios of urinary immunoglobulin G, transferrin, ceruloplasmin, albumin, and α2 macroglobulin to urinary creatinine in daytime and nighttime urine samples, respectively

parameters by χ^2 test revealed no statistically significant differences when compared with identical normal distributions. Nighttime U-IgG/Cr, U-Tf/Cr and U-CRL/Cr were significantly higher in diabetic patients than in controls by student's *t*-test and only nighttime U-IgG/Cr was p<0.05 by Mann–Whitney's U test although there were no differences in these daytime ratios between controls and diabetic patients. Both daytime and nighttime U-Alb/Cr ratios were significantly higher in diabetic patients than in controls by Student's *t*-test although significant difference in nighttime U-Alb/Cr was revealed by Mann–Whitney's U test. Neither daytime nor nighttime U-A2/Cr differed between the two groups. Absolute values of DIs of U-IgG/Cr, U-Tf/Cr and U-CRL/Cr were significantly smaller in diabetic patients than in controls (p=0.0004, p=0.02, and p=0.001, respectively). However, there were no differences between groups regarding DIs of U-Alb/Cr, U-A2/Cr (**Table 1**).

Fig. 1 illustrates correlations between DIs of SBP and those of U-IgG/Cr, U-Tf/Cr, U-CRL/Cr, U-Alb/Cr and U-A2/Cr. Strong, statistically significant correlations between DI of SBP and those of U-IgG/Cr, U-Tf/Cr and U-CRL/Cr (r=0.613, p=0.0009; r=0.415, p=0.0352, and r=0.506, p=0.0083, respectively) were found in diabetic patients, whereas these close relationships were not found in controls. In contrast, no correlation between DI of U-Alb/Cr and that of SBP was found (r=0.306, p=0.1285) even in diabetic patients. Furthermore, DI of U-A2/Cr was not significantly correlated with DI of SBP in either controls or diabetic patients (r=0.049, p=0.836 and r=0.227, p=0.2655, respectively). No correlation between HbA1c and DI of BP was found in either controls or diabetic patients. Additionally, no correlation between HbA1c and DI of U-Alb/Cr, U-IgG/Cr, U-Tf/Cr, U-CRL/Cr and U-A2/Cr was found in either controls or diabetic patients.

Discussion and Conclusions

The present study showed strong correlations between DIs of U-IgG/Cr, U-Tf/Cr, U-CRL/Cr and that of SBP in normoalbuminuric diabetic patients, but not in controls whereas DIs of U-Alb/Cr and U-A2/Cr did not have such a close relationship with DI of SBP in either group. The present findings indicate that, in normoalbuminuric diabetic patients, urinary excretion of SPPs are influenced to a greater extent than urinary excretion of Alb and A2 by systemic BP changes. It appears that these close relationships

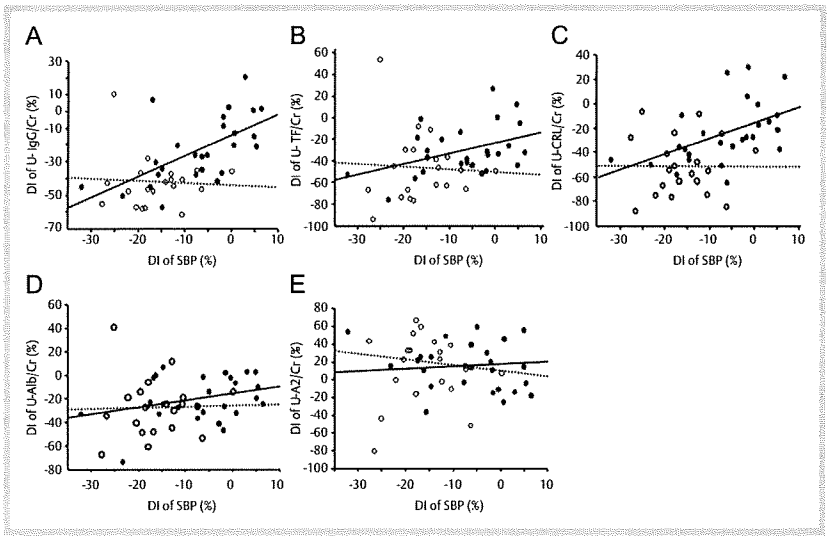

Fig. 1 Relationships between diurnal changes in systolic blood pressure and diurnal changes in urinary excretions of immunoglobulin G (**A**), transferrin (**B**), ceruloplasmin (**C**), albumin (**D**), and α2 macroglobulin (**E**) in control subjects and normoalbuminuric type 2 diabetic patients. White circles, control subjects; black circles, diabetic patients. U-IgG/Cr, U-Tf/Cr, U-CRL/Cr, U-Alb/Cr, and U-A2/Cr represent ratios of urinary immunoglobulin G, transferrin, ceruloplasmin, albumin, and α2 macroglobulin to urinary creatinine in urine samples, respectively. Dashed line, regression line of control subjects; solid line, regression line of diabetic patients. DI: diurnal index (% of [nighttime mean–daytime mean]/daytime mean). **A**: control subjects, r=0.06 (p=0.8029); diabetic patients, r=0.613 (p=0.0009); **B**: control subjects, r=0.055 (p=0.8191); diabetic patients, r=0.415 (p=0.0352); **C**: control subjects, r=0.002 (p=0.9922); diabetic patients, r=0.506 (p=0.0083); **D**: control subjects, r=0.028 (p=0.9067); diabetic patients, r=0.306 (p=0.1285); **E**: control subjects, r=0.049 (p=0.836); diabetic patients, r=0.227 (p=0.2655).

between changes of systemic BP and those of SPPs are induced by diabetic state.

In people without diabetes, renal hemodynamics is regulated to maintain GCP in a narrow range [10]. Therefore, changes in systemic BP are not transmitted to the glomerular capillaries, consistent with the present findings that no correlation between DI of urinary excretion of SPPs and SBP was observed in controls. However, in the diabetic state, slight elevation of systemic blood pressure (BP) may easily transmit to the glomerular capillaries through dilation of afferent arterioles, inducing increased GCP [8–10]. Our recent study of normoalbuminuric diabetic patients revealed that low-dose losartan reversibly decreased urinary excretion of SPPs without changes in urinary excretion of Alb or A2 and that systemic BP change induced by low-dose losartan correlated with changes in urinary SPP excretion but not with urinary excretion of Alb or A2 [15]. Taking together, these findings suggest that, in the kidneys of diabetic normoalbuminuric patients, the tendency for GCP lability induced by afferent arteriole dilation following systemic BP changes may be clinically detected more sensitively by changes in urinary excretion of SPPs than by changes in excretion of Alb or A2.

Proteinuria in diabetic nephropathy has been attributed to three main factors: loss of glomerular charge selectivity [21–23], impairment of glomerular pore size selectivity [23,24], and intra-renal hemodynamic changes, such as the above-mentioned changes in GCP [8–10,25]. Our present findings do not seem to be explained by loss of glomerular charge selectivity because parallel changes in urinary excretions of SPPs were found despite variation in their pIs (IgG, 7.4; Tf, 5.7; CRL, 4.4).

To explain transglomerular plasma protein passage, Deen et al. [26] proposed "the isoporous + shunt model" in which a large portion of the glomerular capillary wall is assumed to be perforated by restrictive pores of identical radii (29–31 A) and a small portion by large nondiscriminatory pores (the shunt pathway, pore size is assumed as 110–115 A) [27]. If glomerular pore size selectivity is impaired, implying that an increased proportion of proteins is filtered through the shunt pathway, urinary A2 excretion may be assumed to be easily influenced by changes in GCP. This idea is supported by findings of our recent study that urinary A2, Alb, IgG and CRL were decreased in parallel in response to combination therapy of glycemic control, low-protein diet and angiotensin-converting enzyme inhibitors in microalbuminuric diabetic patients [21]. It is also supported by a study of neutral dextran clearance showing that impaired size selectivity may be initiated from microalbuminuric state in diabetic patients [24]. Therefore, our present finding that changes in systemic BP correlate with changes in urinary excretion of SPPs, but not with those of A2 cannot be plausibly explained by impaired glomerular size selectivity.

The absence of correlation between change in systemic BP and that of U-Alb/Cr in both diabetic patients and controls in the present study, confirming the results of a previous study in normoalbuminuric type 1 diabetic patients [28], cannot be explained by these ideas, since it seems likely that Alb with its MR of 36 A would have passed through the nondiscriminatory pores and would have increased flux through these large pores in the presence of increased GCP. One explanation for this finding is preferential tubular reabsorption of Alb. Recent studies reveal that certain fraction of Alb is reabsorbed by proximal tubules [29] and that albuminuria may be caused by impairment of reabsorption and degradation after glomeruli [30,31]. Taken together, in the present normoalbuminuric diabetic patients, intact tubular handling of Alb may abolish changes in its urinary excretion even if altered GCP caused fluctuations in its glomerular flux. On the other hand, the degree of potential tubular handling of IgG, Tf, and CRL may not completely stabilize changes in urinary excretion of IgG, Tf, and CRL in response to changes in renal hemodynamics, considering the results of our APL study in

healthy participants showing increased urinary excretion of SPPs without changes in albuminuria [13]. The phenomena that urinary Alb excretion is unresponsive to the changes in systemic BP compared with urinary excretion of IgG, Tf and CRL in our normoalbuminuric diabetic patients may be explained by differences in tubular handling.

The nighttime excretion rates of SPPs were higher with tendencies toward statistically significant differences in diabetic patients although there were no differences between controls and diabetic patients for nighttime BP levels. More numbers of subjects like our recent studies [7] seem to be necessary to have definitive, statistically significant differences in these urinary proteins between normoalbuminuric diabetic patients and controls. In the present study, the percentage of 'nondippers' was significantly higher in normoalbuminic diabetic patients than in controls. As to diabetic neuropathy, parasympathetic fibers reportedly tend to be affected first [32], resulting in nocturnal sympathetic predominance. Furthermore, increased urinary IgG excretion is reportedly induced by exogenous norepinephrine administration in controls and type 1 diabetic patients, which may cause an increase in GCP [33]. When these findings are considered collectively, it is plausible that increases in nighttime urinary SPPs excretion in normoalbuminuric diabetic patients may be explained in part by this autonomic dysfunction.

On the basis of above mentioned autonomic nerve dysfunction in our diabetic patients, it is also plausibly comprehensible that they had a smaller diurnal change in systemic BP (**Table 1**) and may have higher GCP in nighttime, resulting in higher levels of nighttime urinary SPPs excretion with relation to lower levels of diurnal change in urinary SPPs (**Table 2**), when compared with controls. However, due to GCP lability induced by dilatation of afferent arterioles in diabetic state [10], even small diurnal change in systemic BP would be directly transmitted to GCP, resulting in a closer correlation between DI of SBP and that of urinary excretion of SPP despite of lower absolute values of these parameters. On the other hand, in control subjects, the appropriate constriction and dilatation of glomerular afferent arterioles according to systemic BP change [10] may be a cause of no correlation between DIs of urinary excretion of SPPs and that of SBP, despite of higher absolute values of these parameters.

Jafer et al. [34] reported that the albumin creatinine ratio is much less sensitive in an indo-Asian population to predict 24-h urinary albumin excretion of >30 mg/day. However, 24-h urine Alb excretion of all participants are less than 30 mg/day on the day of ABPM measurement. All of our diabetic patients of the present study had definite normoalbuminuria.

In the present study, both day and night U-Alb/Cr in diabetic patients were higher even within normoalbuminuric rang than in controls subjects (**Table 2**). Further, the proportion of nondippers was approximately four times higher in diabetic patients than in controls (61.5% and 15.0%, respectively). These clinical characteristics of our patients would be consistent with an intermediate phase in the evolution of MA documented by Poulsen et al. [35]. They reported that the transition from normoalbuminuria to even modest MA in type 1 diabetic patients is associated with initial increased urinary Alb excretion and significant BP increases in 24-h ABPM levels during follow-up period not but with initial 24-h ABPM levels or BPs measured in clinics. On the other hand, we previously reported that the initial increased urinary SPPs in overnight urine samples predict future development of MA [7]. In the present study, we have found close relationships between changes in urinary excretion of SPPs and the diurnal index of 24-h systolic ABPM, indicating urinary SPPs may increase with close relationships with systemic BP change. However, mutual causal relationships among these clinical parameters in relation with MA development are still unknown. Serial prospective studies of our patients should be warranted to answer the issue.

In conclusion, we found that changes in urinary excretions of SPPs have close relationships with changes in systemic BP in normoalbuminuric diabetic patients, while urinary excretions of Alb and A2 do not have such relationships. From these findings, the tendency for GCP lability due to afferent arteriole dilation following systemic BP changes in the diabetic state may be more sensitively detected by measuring urinary excretions of SPPs rather than Alb in normoalbumiuric diabetic patients. For further confirmation of this hypothesis, it would be useful to elucidate in similar patients and controls whether other interventions directed at altering BP are directly related to changes in urinary excretions of SPPs but not to change in albuminuria.

References

1 *Gross JL, de Azevedo MJ, Silveiro SP, Canani LH, Caramori ML, Zelmanovitz T.* Diabetic nephropathy: diagnosis, prevention, and treatment. Diabetes Care 2005; 28: 164–176

2 *Jerums G, Allen TJ, Cooper ME.* Triphasic changes in selectivity with increasing proteinuria in type 1 and type 2 diabetes. Diabet Med 1989; 6: 772–779

3 *Narita T, Fujita H, Koshimura J, Meguro H, Kitazato H, Shimotomai T, Kagaya E, Suzuki K, Murata M, Usami A, Ito S.* Glycemic control reverses increases in urinary excretion of immunoglobulin G and ceruloplasmin in type 2 diabetic patients with normoalbuminuria. Horm Metab Res 2001; 33: 370–378

4 *Bernard AM, Ouled Amor AA, Goemaere Vanneste J, Antonie JL, Lauwerys RR, Lambert A, Vandeleene B.* Microtransferrinuria is a more sensitive indicator of early glomerular damage in diabetes than microalbuminuria. Clin Chem 1988; 34: 1920–1921

5 *Kazumi T, Hozumi T, Ishida Y, Ikeda Y, Kishi K, Hayakawa M, Yoshino G.* Increased urinary transferrin excretion predicts miroalbuminuria in patients with type 2 diabetes. Diabetes Care 1999; 22: 1176–1180

6 *Yamazaki M, Ito S, Usami A, Tani N, Hanyu O, Nakagawa O, Nakamura H, Shibata A.* Urinary excretion rate of ceruloplasmin in non-insulin dependent diabetic patients with different stage of nephropathy. Eur J Endocrinol 1995; 132: 681–687

7 *Narita T, Hosoba M, Kakei M, Ito S.* Increased urinary excretions of immunoglobulin G, ceruloplasmin, and transferrin predict development of microalbuminuria in patients with type 2 diabetes. Diabetes Care 2006; 29: 142–144

8 *Hostetter TH, Troy JL, Brenner BM.* Glomerular hemodynamics in experimental diabetes mellitus. Kidney Int 1981; 19: 410–415

9 *Hostetter TH, Rennke HG, Brenner BM.* The case for intrarenal hypertension in the initiation and progression of diabetic and other glomerulopathies. Am J Med 1982; 72: 375–380

10 *Arima S, Ito S.* The mechanisms underlying altered vascular resistance of glomerular afferent and efferent arterioles in diabetic nephropathy. Nephrol Dial Transplant 2003; 18: 1966–1969

11 *King AJ, Levey AS.* Dietary protein and renal function. J Am Soc Nephrol 1993; 3: 1723–1737

12 *Woods LL.* Mechamisms of renal hemodynamic regulation in response to protein feeding. Kidney Int 1993; 44: 659–675

13 *Narita T, Kitazato H, Koshimura J, Suzuki K, Murata M, Ito S.* Effects of protein meals on the urinary excretion of various plasma proteins in healthy subjects. Nephron 1999; 81: 398–405

14 *Koshimura J, Narita T, Sasaki H, Hosoba M, Yoshioka N, Shimotomai T, Fujita H, Kakei M, Ito S.* Urinary excretion of transferrin and orosomucoid are increased after acute protein loading in healthy subjects. Nephron Clin Pract 2005; 100: c33–c37

15 *Narita T, Hosoba M, Miura T, Sasaki H, Morii T, Fujita H, Kakei M, Ito S.* Low dose of losartan decreased urinary excretions of IgG, transferrin, and ceruloplasmin without reducing albuminuria in normoalbuminuric type 2 diabetic patients. Horm Metab Res 2008; 40: 292–295

16 *Japan Diabetes Society.* Diet therypy. In Treatment Guide for Diabetes. Tokyo: Bunkodo; 2007; 34–37

17 *Bosch JP, Saccaggi A, Lauer A, Ronco C, Belledonne M, Glabman S.* Renal functional reserve in humans. Am J Med 1983; 75: 943–950
18 *Nakamura H, Ebe N, Ito S, Shibata A.* Renal effects of different types of protein in healthy volunteer subjects and diabetic patients. Diabetes Care 1993; 16: 1071–1075
19 *Kontessis P, Jones S, Dodds R, Trevisan R, Nosadini R, Fioretto P, Borsato M, Sacerdoti D, Viberti G.* Renal, metabolic and hormonal responses to ingestion of animal and vegetable proteins. Kidney Int 1990; 38: 136–144
20 *Ito S, Usami A, Yamazaki M, Shibata A.* A radioimmuno-metric assay for urinary α2-macroglobulin. Tohoku J Exp Med 1995; 176: 137–147
21 *Narita T, Koshimura J, Suzuki K, Murata M, Meguro H, Fujita H, Kitazato H, Ito S.* Effects of short-term glycemic control, low protein diet and administration of enalapril on renal hemodynamics and protein permselectivity in type 2 diabetic patients with microalbuminuria. Tohoku J Exp Med 1999; 189: 117–133
22 *Nakamura Y, Myers BD.* Charge selectivity of proteinuria in diabetic glomerulopathy. Diabetes 1988; 37: 1202–1211
23 *Deckert T, Kofoed-Enevoldsen A, Vidal P, Nørgaard K, Andreasen HB, Feldt-Rasmussen B.* Size- and charge selectivity of glomerular filtration in type 1 (insulin- dependent) diabetic patients with and without albuminuria. Diabetologia 1993; 36: 244–251
24 *Scandling JD, Myers BD.* Glomerular size selectivity and microalbuminuria in early diabetic glomerular disease. Kidney Int 1992; 41: 840–846
25 *Anderson S, Brenner BM.* Pathogenesis of diabetic nephropathy: hemodynamic considerations. Diabetes Metab Rev 1988; 4: 163–177
26 *Deen WM, Bridges CR, Brenner BM, Myers BD.* Heteroporous model of glomerular size selectivity: application to normal and nephrotic humans. Am J Physiol 1985; 249: F374–F389
27 *Tencer J, Frick IM, Öqvist B, Alm P, Rippe B.* Size selectivity of the glomerular barrier to high molecular weight proteins: the upper size limitation of the shunt pathways. Kindey Int 1998; 53: 709–715
28 *Hansen PM, Goddijn PP, Kofoed-Enevoldsen A, van Tol KM, Bilo HJ, Deckert T.* Diurnal variation in glomerular charge selectivity, urinary albumin excretion and blood pressure in insulin-dependent diabetic patients. Kidey Int 1995; 48: 1559–1562
29 *Osicka TM, Houlihan CA, Chan JG, Comper WD.* Albuminuria in patients with type 1 diabetes is directly linked to changes in the lysosome-mediated degradation of albumin during renal passage. Diabetes 2000; 49: 1579–1584
30 *Russo LM, Bakris GL, Comper WD.* Renal handling of albumin: a critical review of basic concepts and perspective. Am J Kidey Dis 2002; 39: 899–919
31 *Tojo A, Onozato ML, Ha H, Kurihara H, Sakai T, Goto A, Fujita T, Endou H.* Reduced albumin reabsorption in the proximal tubule of early-stage diabetic rats. Histochem Cell Biol 2001; 116: 269–276
32 *Wieling W, Borst C, van Dongen Torman MA, van der Hofstede JW, van Brederode JF, Endert E, Dunning AJL.* Relationship between impaired parasympathetic and sympathetic cardiovascular control in diabetes mellitus. Diabetologia 1983; 24: 422–427
33 *Hoogenberg K, Sluiter WJ, Navis G, Van Haeften TW, Smit AJ, Reitsma WD, Dullaart RPF.* Exogenous norepinephrine induces an enhanced microproteinuric response in microalbuminuric insulin-dependent diabetes mellitus. J Am Soc Nephrol 1998; 9: 643–654
34 *Jafar TH, Nishi C, Juanita H, Levey AS.* Use of albumin creatinin ratio and urine albumin concentration as a screening test for albuminuira in an Indo-Asian population. Neohrol Dial Transplant 2007; 22: 2194–2200
35 *Poulsen PL, Hansen KW, Mogensen CE.* Ambulatory blood pressure in the transition from normo-to microalbuminuria. Diabetes 1994; 43: 1248–1253

Leukemia Research 33 (2009) 924–928

Contents lists available at ScienceDirect

Leukemia Research

journal homepage: www.elsevier.com/locate/leukres

The anti-apoptotic role of the unfolded protein response in Bcr-Abl-positive leukemia cells

Atsuko Tanimura[a], Toshiaki Yujiri[a,*], Yoshinori Tanaka[a], Masayuki Hatanaka[a], Noriyuki Mitani[a], Yukinori Nakamura[a], Kazutoshi Mori[b], Yukio Tanizawa[a]

[a] Department of Bio-Signal Analysis, Yamaguchi University Graduate School of Medicine, Ube, Yamaguchi 755-8505, Japan
[b] Department of Biophysics, Graduate School of Science, Kyoto University, Kyoto, Japan

ARTICLE INFO

Article history:
Received 29 May 2008
Received in revised form 17 December 2008
Accepted 24 January 2009
Available online 23 February 2009

Keywords:
Unfolded protein response
Bcr-Abl
Apoptosis

ABSTRACT

To define the role of the unfolded protein response (UPR) in leukemogenesis, we investigated UPR activation in the cells expressing the representative oncogene Bcr-Abl (B-A). The expression of UPR-related proteins and mRNAs, namely, X-box-binding protein (XBP1) and glucose-regulated protein 78 (GRP78) was increased in B-A. UPR inhibition using inositol-requiring enzyme 1α (IRE1α) or activating transcription factor 6 (ATF6) dominant-negative mutants diminished the ability of Bcr-Abl to protect the cells from etoposide- and imatinib-induced apoptosis. We also noted that the expression of UPR-related genes in primary leukemia cells from Philadelphia chromosome (Ph)-positive cells was higher than that in the control by quantitative RT-PCR assay. Thus, our results suggested that UPR is a downstream target of Bcr-Abl and plays an anti-apoptotic role in Ph-positive leukemia cells.

1. Introduction

The Bcr-Abl fusion protein plays a central role in chronic myeloid leukemia (CML) and Philadelphia chromosome (Ph)-positive acute leukemia. The molecular mechanism of leukemogenesis by Bcr-Abl has been the focus of intensive research over several decades. The transformation of hematopoietic cells by Bcr-Abl involves the assembly of multiprotein complexes and phosphorylation of several substrates, leading to the activation of signal transduction pathways that generate proliferative and anti-apoptotic signals.

The accumulation of unfolded proteins in the lumen of the endoplasmic reticulum (ER) induces a coordinated adaptive program termed as the unfolded protein response (UPR). The UPR alleviates stress by upregulating protein folding in the ER and inhibiting protein synthesis. In mammalian cells, the UPR is initiated by diverse signaling pathways whenever protein folding in the ER is compromised. Physiological conditions that induce the UPR by causing protein misfolding include the differentiation and development of professional secretory cells such as plasma cells or pancreatic β cells; altered metabolic conditions such as glucose deprivation and ischemia; mutations in the genes encoding secretory or transmembrane proteins, which are normally folded in the ER, such as insulin; and infection by certain pathogens, such as hepatitis C.

Although a number of studies have reported UPR activation in a variety of solid tumors, the UPR in cancers remains poorly characterized. It is not known whether UPR activation in cancers is solely due to microenvironmental stress or other mechanisms [1]. Moreover, the influence of the UPR on leukemogenesis remains largely uninvestigated. Here, we showed the constitutive activation of UPR in Bcr-Abl-expressing cells and demonstrated that the UPR plays a role in the anti-apoptotic effect of Bcr-Abl.

2. Materials and methods

2.1. Cell culture

32Dcl3 mouse myeloid cells (RIKEN Cell Bank, Saitama, Japan) were cultured in RPMI 1640 medium supplemented with 10% FBS and 1 ng/ml recombinant murine IL-3. The vectors pZeo-p210 Bcr-Abl (B-A), pZeo-c-Abl (Abl), and pZeoSV2 (Mock) (Invitrogen, Carlsbad, CA, USA) were stably transfected into the 32Dcl3 cells using Nucleofector (Amaxa, Inc., Gaithersburg, MD, USA). The complementary DNAs encoding p210 Bcr-Abl and c-Abl were of human origin. Bcr-Abl-expressing cells were selected and cultured following IL-3 withdrawal. Abl and Mock were selected using 600 μg/ml Zeocin and maintained with 350 μg/ml Zeocin (Invitrogen). The expression plasmid for IRE1α lacking the sequence of kinase and ribonuclease domain (IRE1 DN) [2] or for ATF6α lacking the sequence of activation domain (amino acids 171–373) (ATF6 DN) [3] was stably transfected into B-A and Mock. Stable B-A or Mock transformants were selected using 300 μg/ml or 1.2 mg/ml geneticin (Invitrogen), respectively. The stably transfected cells were used as uncloned pools for the experiments in order to avoid the effects of clonal selection.

2.2. Patients

This study was approved by the Institutional Review Board, and informed consent was obtained from all the patients and healthy controls. Samples obtained

* Corresponding author. Tel.: +81 836 222251; fax: +81 836 222342.
E-mail address: yujirit@yamaguchi-u.ac.jp (T. Yujiri).

0145-2126/$ – see front matter © 2009 Elsevier Ltd. All rights reserved.
doi:10.1016/j.leukres.2009.01.027

from 8 Ph-positive acute lymphoblastic leukemia patients (4, bone marrow (BM); 4, peripheral blood (PB)) and 12 healthy controls (7, BM; 5, PB) were analyzed. Mononuclear cells were collected using Lymphoprep (Axis-Shield, Oslo, Norway).

2.3. Immunoblot analysis

The following antibodies were used for immunoblot analysis; anti-Crk-L (sc-319) and anti-XBP1 (sc-7160) (Santa Cruz Biotechnology, Santa Cruz, CA, USA), anti-phospho-eIF2α (Ser51) and anti-eIF2α (Cell Signaling Technology, Inc., Beverly, MA, USA), anti-KDEL (SPA-827) (Stressgen, Ann Arbor, MI, USA), anti-c-Abl (OP20) (Calbiochem, San Diego, CA, USA), anti-GAPDH (MAB374) (Chemicon International, Inc., Temecula, CA, USA), and anti-Nucleoporin p62 (BD Biosciences, San Jose, CA, USA).

2.4. Luciferase assay

HEK293T cells with the ER stress response element (ERSE) or unfolded protein response element (UPRE) reporter [4] were transiently cotransfected with pZeo-p210 Bcr-Abl, pZeo-c-Abl, or an empty vector alone and the β-galactosidase expression plasmid pZeoSV2/lacZ using FuGENE6 (Roche Diagnostics, Indianapolis, IN, USA). After 48 h of incubation, luciferase activity was measured using the PicaGene reagent kit (Toyo Inki, Tokyo, Japan) according to the manufacturer's instructions and normalized to the corresponding β-galactosidase activity levels. 32Dcl3 cells stably expressing Bcr-Abl (B-A) or the empty vector (Mock) were analyzed by a luciferase assay using the ERSE or UPRE reporter with the pGL4.74 vector (Promega, Madison, WI, USA) as a normalized control.

2.5. Quantitative reverse transcription-polymerase chain reaction assay (RT-PCR) assay

Total RNA from the mononuclear cells was extracted using ISOGEN (Nippon Gene Co. Ltd., Tokyo, Japan) according to the manufacturer's instructions. Total RNA was subjected to reverse transcription with Superscript II Reverse Transcriptase (Invitrogen) according to the manufacturers' instructions. Quantitative RT-PCR assay of the indicated genes was performed using a QuantiTect SYBR Green PCR kit (Qiagen, Hilden, Germany) with a LightCycler system (Roche Diagnostics). The primer sequences for each of the murine UPR-related genes are as follows: spliced form of XBP1, 5′-gctgagtccgcagcaggtgc-3′ and 5′-catgacagggtccaacttgtccag-3′; GRP78, 5′-gacatttgccccagaagaaa-3′ and 5′-ctcatgacattcagtccagca-3′;CHOP, 5′-cctagcttggctgacagagg-3′ and 5′-ctgctccttctccttcatgc-3′; P58IPK, 5′-ccttatcggacagtcc-ttcg-3′ and 5′-tcagagtcctgatttcatcttca-3′; ERdj4, 5′-cttaggtgtgccaaagtctgcc-3′ and 5′-ccgagagtgtttcatacgcttctg-3′; and GAPDH, 5′-ggcattgctctcaatgacaa-3′ and 5′-atg-taggccatgaggtccac-3′. The primer sequences for each of the human UPR-related genes are as follows: spliced form of XBP1, 5′-tgagtccgcagcaggtgc-3′ and 5′-tggcaggctctggggaag-3′; GRP78, 5′-gagttcttcaatggcaagg-3′ and 5′-ggggaca-tacatcaagcag-3′; EDEM, 5′-tctcctctaccaggcaacc-3′ and 5′-cggtcttctgtggacttgtc-3′; CHOP, 5′-cctatgtttcacctcctgg-3′ and 5′-tgacctctgctggttctg-3′; and β-actin, 5′-caag-agatggccacggctgct-3′ and 5′-tccttctgcatcctgtcggca-3′.

The calculated concentration was normalized to the expression level of β-actin or GAPDH mRNA.

2.6. Apoptosis assay

The cells were treated with 20 μM etoposide or 1.5 μM imatinib and incubated for 14 or 16 h, respectively. To measure the extent of apoptosis, the cells were stained using an Annexin-V-FLUOS staining kit (Roche Diagnostics). Cytomics FC500 (Beckman Coulter Inc., Fullerton, CA, USA) was used for flow cytometric analysis.

3. Results and discussion

To determine whether the Bcr-Abl oncoprotein altered the UPR, we evaluated the expression of UPR-related proteins. Bcr-Abl, c-Abl, or an empty vector was stably transfected into 32Dcl3 cells. Bcr-Abl-expressing cells (B-A) showed an upward shift in CrkL, a tyrosine-phosphorylated substrate by Bcr-Abl tyrosine kinase (Fig. 1a). The expression of the UPR-related proteins, namely, glucose-regulated protein 78 (GRP78) and the phosphorylated α-subunit of eukaryotic translation initiation factor 2α (eIF2α), was elevated in B-A as compared to that in c-Abl-transfected (Abl) or empty vector-transfected (Mock) cells under basal conditions (Fig. 1a). To confirm UPR upregulation, the cells were treated with an ER stress activator, thapsigargin. All the cells showed elevated levels of GRP78 and phosphorylated eIF2α after treatment with thapsigargin. The upregulated expression of UPR-related proteins was consistently observed in B-A as compared to Mock and Abl (Fig. 1a). Treatment of the cells with another ER stress activator, tunicamycin produced the same result (data not shown). GRP78

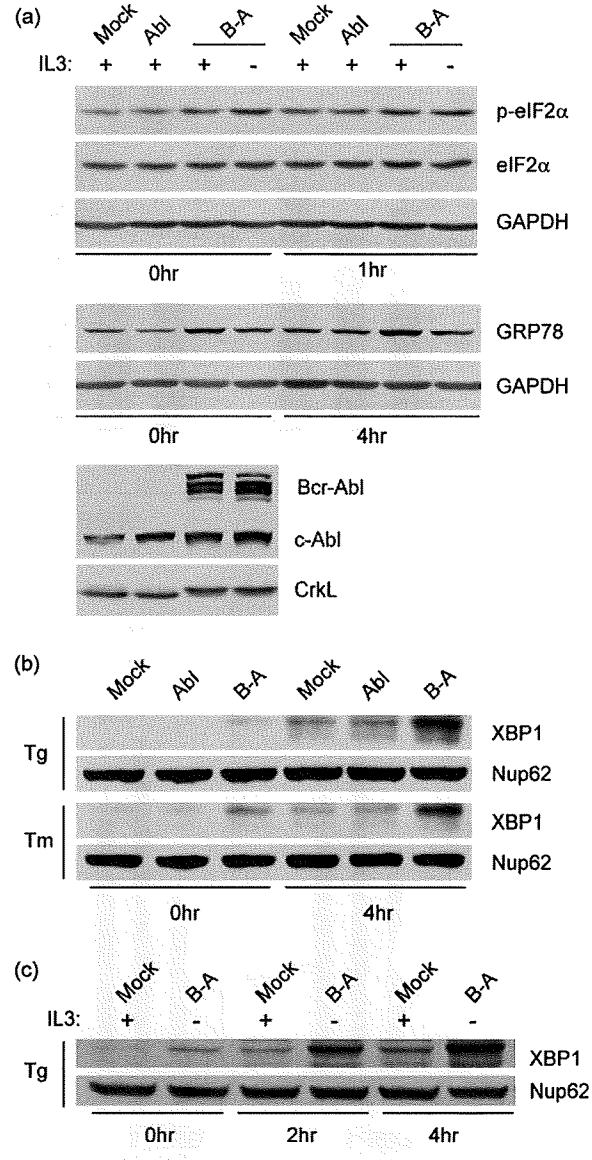

Fig. 1. The expression of UPR-related proteins is upregulated in Bcr-Abl-expressing cells. (a) B-A, Abl, and Mock were produced by transfecting 32Dcl3 cells with the vectors pZeo-p210 Bcr-Abl, pZeo-c-Abl, and pZeoSV2, respectively. The cells were treated with 600 nM thapsigargin for the indicated time periods. Immunoblot analysis was performed with the following antibodies; anti-CrkL, anti-eIF2α, anti-phospho-eIF2α (Ser51), anti-KDEL, anti-c-Abl, and anti-GAPDH. (b) XBP1 expression in nuclear lysates was analyzed using anti-XBP1 antibody. The cells were treated with either 600 nM thapsigargin (Tg) or 2 μg/ml tunicamycin (Tm) for 4 h. Nucleoporin p62 was used as the loading control. All the cells were cultured in the presence of IL-3. (c) XBP1 expression in nuclear lysates was examined. The cells were treated with 600 nM thapsigargin for the indicated time periods.

is a key regulator of the UPR. As a Ca^{2+}-binding molecular chaperone in the ER, GRP78 maintains ER homeostasis, suppresses stress-induced apoptosis, and controls UPR signaling. The phosphorylation of eIF2α at Ser51 is an early event associated with the downregulation of protein synthesis at the level of translation and initiation of a transcriptional program. This constitutes a potent mechanism to overcome various stress conditions including ER stress. Furthermore, B-A in the presence or absence of IL-3 showed higher levels of the X-box-binding protein 1 (XBP1) in the nuclear extract than Abl or Mock did (Fig. 1b and c). The treatment with thapsigargin or tunicamycin clarified that nuclear XBP1 was increased by drug-induced ER stress and was consistently elevated in B-A as compared to that in Mock or Abl either in the presence or absence of IL-3 (Fig. 1b and c). XBP1 pre-messenger RNA is

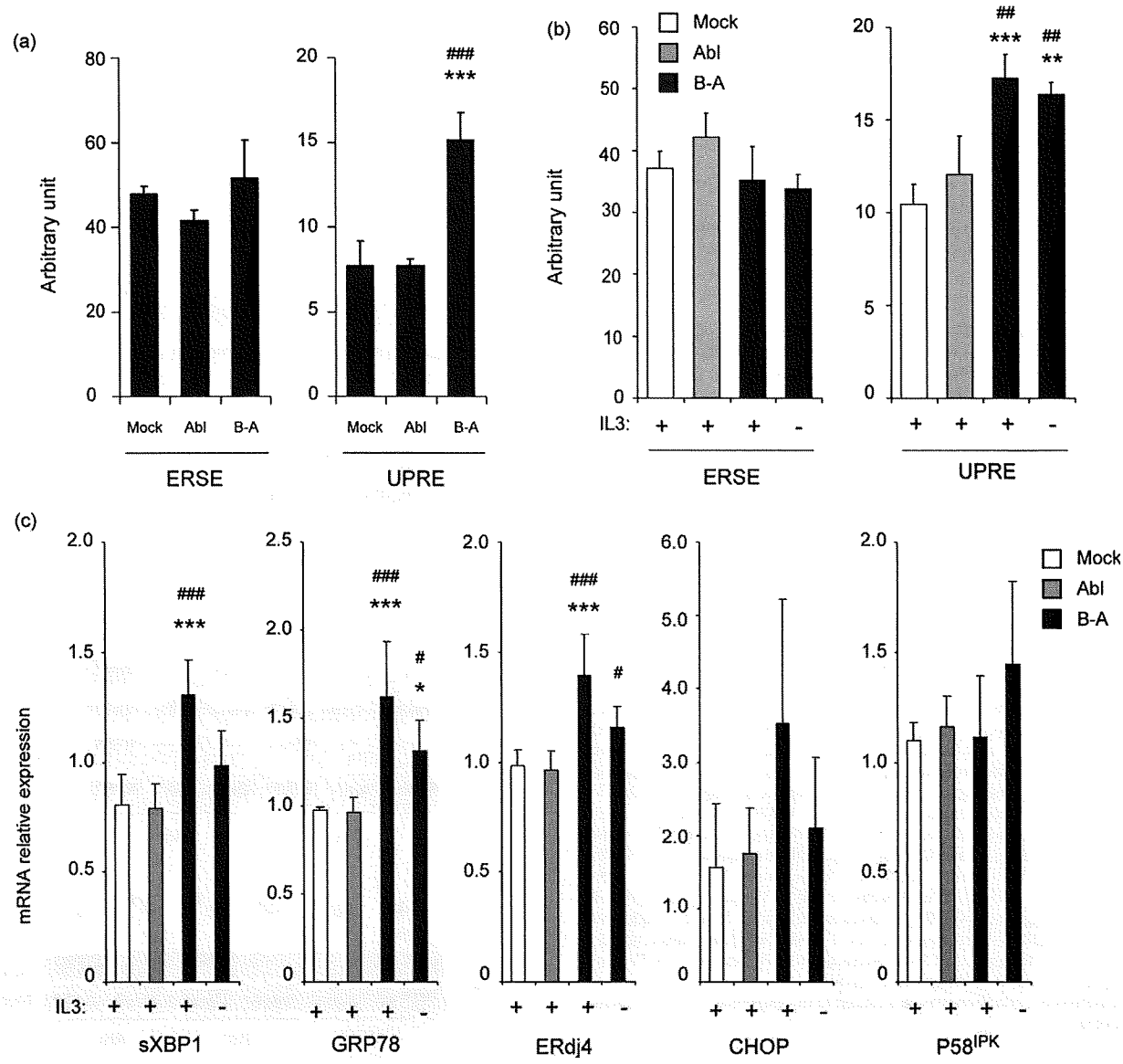

Fig. 2. Bcr-Abl enhances the expression of UPR-related mRNAs. (a) HEK293T cells with the ERSE or UPRE reporter were transiently cotransfected with the vectors pZeo-p210 Bcr-Abl (B-A), pZeo-c-Abl (Abl), or an empty vector alone (Mock) and the β-galactosidase expression plasmid pZeoSV2/lacZ. The data were statistically analyzed by one-factor ANOVA, followed by Fisher's PLSD test. The means ± S.D. of 3 independent experiments are shown. (b) 32Dcl3 cells stably expressing Bcr-Abl (B-A), c-Abl (Abl) or an empty vector (Mock) were analyzed by a luciferase assay using the ERSE or UPRE reporter. Statistical analyses were performed using one-factor ANOVA followed by Fisher's PLSD test. The means ± S.D. of 3 independent experiments are shown. (c) 32Dcl3 cells stably expressing Bcr-Abl (B-A), c-Abl (Abl), and an empty vector (Mock) were analyzed by a quantitative RT-PCR assay of the indicated genes. Statistical analyses were performed using one-factor ANOVA followed by Fisher's PLSD test. The means ± S.D. of 4 independent experiments are shown. $^{*}P<0.05$, $^{**}P<0.005$, $^{***}P<0.0005$, compared to Mock. $^{\#}P<0.05$, $^{\#\#}P<0.005$, $^{\#\#\#}P<0.0005$, compared to Abl.

converted to mature mRNA by unconventional splicing that is mediated by the endonuclease inositol-requiring enzyme 1 (IRE1). The transcription factor protein XBP1 spliced, which is translated from mature XBP1 mRNAs, contains a nuclear localization signal and a transcriptional activation domain and activates the transcription of target genes in the nucleus.

To examine whether Bcr-Abl induces the UPR-related transcriptional activity, we performed the luciferase reporter assay. Bcr-Abl, c-Abl, or an empty vector was transiently transfected into HEK293T cells with the ERSE or UPRE reporter construct [4]. ERSE-mediated transcriptional activity did not considerably differ between Mock, Abl, and B-A. In addition, the nuclear levels of activating transcription factor 6 (ATF6), an ERSE-binding transcription factor, also did not significantly differ between Mock, Abl, and B-A (data not shown). On the other hand, UPRE-mediated transactivation in B-A was significantly increased as compared to that in Mock or Abl (Fig. 2a). Similar results were obtained in the 32Dcl3 cells stably expressing Bcr-Abl in the presence or absence of IL-3 (Fig. 2b). These data suggested that Bcr-Abl-induced UPR was regulated, at least, through UPRE-mediated transcriptional activation. Next, we investigated the expression of UPR-related genes in Bcr-Abl-expressing 32Dcl3 cells. The mRNA expression of the spliced form of XBP1; GRP78; C/EBP-homologous protein-10 (CHOP); ERdj4, a mammalian chaperone that belongs to the HSP40 protein family; and the cochaperone protein p58IPK was analyzed using a quantitative RT-PCR assay. GAPDH mRNA expression was used as a normalized control. The mRNA expression of the spliced form of XBP1, GRP78, and ERdj4 was significantly increased in B-A. Meanwhile, the mRNA expression of CHOP and p58IPK showed no significant increase in B-A (Fig. 2c). Taken together, our data suggested that Bcr-Abl constitutively induced the UPR, which subsequently increased the expression of several UPR-related mRNAs.

We intended to understand the contribution of the UPR to Bcr-Abl-induced leukemogenesis. To define the role of the UPR in

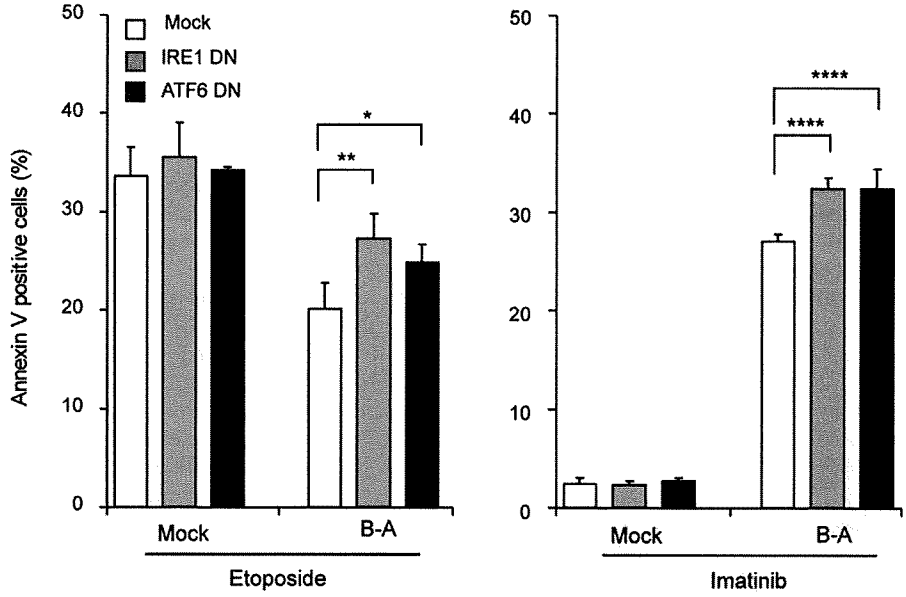

Fig. 3. Dominant-negative mutants of IRE1α and ATF6 reduce the anti-apoptotic effects of Bcr-Abl. The expression plasmid for IRE1α lacking the sequence of the kinase and ribonuclease domains (IRE1 DN) or that for ATF6α lacking the sequence of the activation domain (amino acids 171–373) (ATF6 DN) was stably transfected into cells expressing Bcr-Abl (B-A) and an empty vector (Mock). Apoptosis assay was independently repeated 3 times. The means ± S.D. of 3 independent experiments are shown. Statistical analyses were performed using one-factor ANOVA followed by Fisher's PLSD test. $^{*}P<0.05$; $^{**}P<0.01$; $^{****}P<0.0001$.

Bcr-Abl-expressing cells, the dominant-negative mutants of ATF6 [3] or IRE1α [2] were stably transfected into Mock and B-A. The expression of the dominant-negative ATF6 (ATF6 DN) or IRE1α (IRE1α DN) did not affect the proliferation rate of either Mock or B-A in the presence or absence of IL-3 (data not shown). Thus, the ATF6- or IRE1α-mediated UPR did not exert any effect on Bcr-Abl-induced proliferation or IL-3 dependency. On the other hand, the number of apoptotic cells induced by the genotoxin etoposide was significantly increased in both ATF6 DN- and IRE1α DN-transfected B-A than in empty vector-transfected B-A. Interestingly, treatment with imatinib, a specific Abl tyrosine kinase inhibitor, also resulted in a greater number of apoptotic cells in mutant-transfected B-A than in the control (Fig. 3). Thus, these data suggested that the ATF6- or IRE1α-UPR signaling pathways were associated with the anti-apoptotic effect of the Bcr-Abl oncoprotein. The data obtained from the ATF6 mutant suggested that ATF6

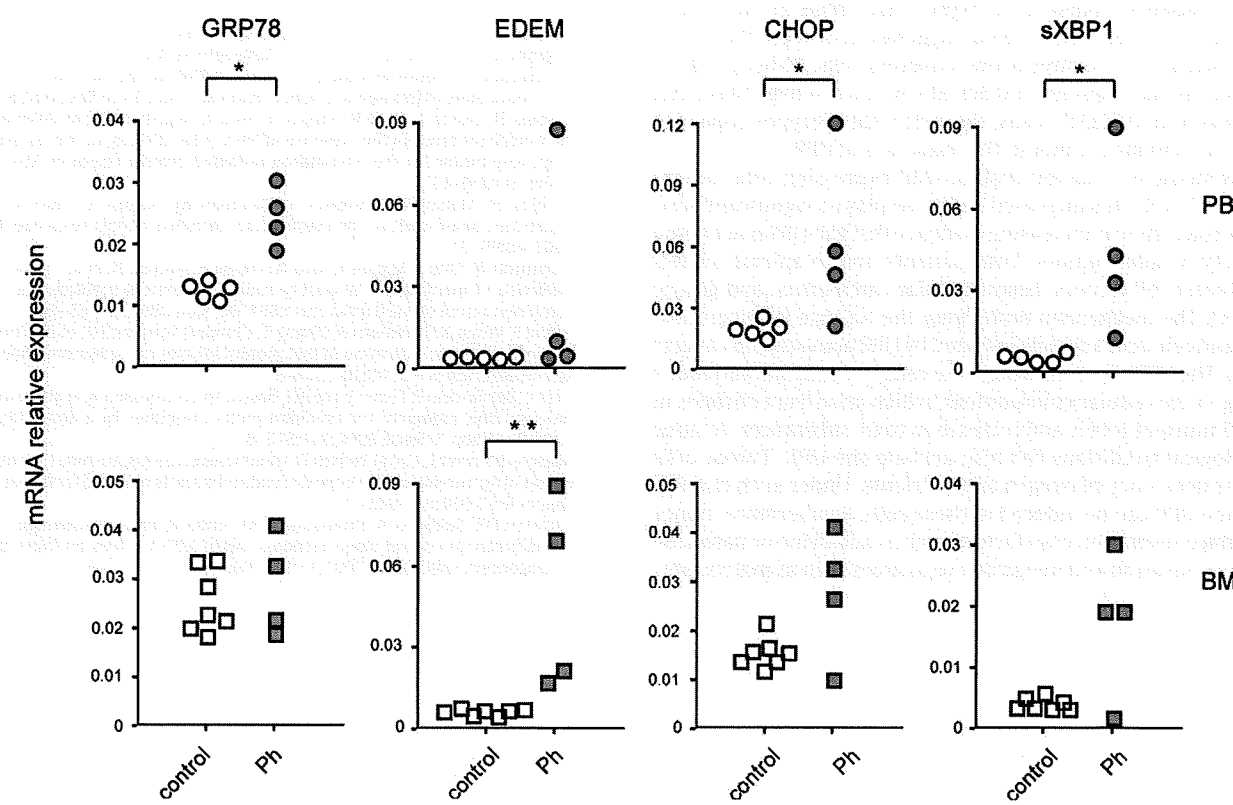

Fig. 4. The levels of UPR-related mRNAs are increased in Ph-positive primary acute leukemia cells. The data were statistically analyzed by Mann–Whitney *U*-test. $^{*}P<0.05$; $^{**}P<0.01$.

was a transcription factor that contributed to the Bcr-Abl-induced cell survival of cells following anticancer drug administration, even though the levels of the nuclear ATF6 protein and ERSE-mediated transactivation were not increased by Bcr-Abl. Recently, ATF6α was reported to heterodimerize with XBP1 for the induction of ER-associated degradation components, a part of the UPR [5]. ATF6 mutant might inhibit the ATF6-XBP1 heterodimerization and eventually decrease UPRE-mediated transactivation. IRE1α mutants lacking the cytosolic effector domain inhibit the activation of XBP1 by inhibiting the ribonuclease activity. Further, they inhibit the autophosphorylation of IRE1α, which in turn induces the formation of the complex of tumor necrosis factor receptor associated factor 2 (TRAF2), apoptosis signal-regulating kinase 1 (ASK1) [6], and Bax/Bak, proapoptotic Bcl-2 family proteins [7]. IRE1α might regulate the Bcr-Abl-induced survival pathway via XBP1 activation, modification of IRE1α-TRAF2-ASK1 signaling, and the IRE1α-Bax-Bak complex formation. Further studies are required to elucidate the mechanisms of Bcr-Abl-IRE1α signaling. Our data also showed that the phosphorylation of eIF2α was constitutively elevated in B-A (Fig. 1). However, the mechanism of eIF2α activation by Bcr-Abl remains to be elucidated. Since the UPR has both protective and destructive roles, it is essential to fully characterize the branches and downstream components of the UPR that are activated in Bcr-Abl-expressing cells.

Finally, we investigated whether primary Ph-positive acute leukemia cells showed UPR activation. We analyzed the mRNA expression of UPR-related genes, namely, GRP78, ER-degradation enhancing α-mannosidase-like protein (EDEM), CHOP, and the spliced form of XBP1, in Ph-positive acute lymphoblastic leukemia cells by real-time RT-PCR analysis. Most of the PB or BM mononuclear cells analyzed were Ph-positive leukemia cells. The mRNA expression of GRP78, CHOP, and the spliced form of XBP1 was significantly increased in the PB leukemia cells and that of EDEM was significantly increased in the BM leukemia cells (Fig. 4). The mRNA expression levels of CHOP and the spliced form of XBP1 in the BM of patients tended to be higher than those in the control BM mononuclear cells. These data suggested that the UPR is activated in primary Ph-positive acute leukemia cells. Although these leukemia cells may express p190 Bcr-Abl in contrast to p210 Bcr-Abl in the transformed 32Dcl3 cells, these Bcr-Abl subtypes appear to function in a similar manner in the induction of UPR.

In this study, we showed that Bcr-Abl-expressing cells exhibit an increased UPR. This increased response plays a significant anti-apoptotic role. There is increasing evidence that the UPR is activated in a variety of solid tumors, from patients and in animal models such as breast cell tumors, hepatocellular carcinomas, and gastric tumors [1]. The mechanism underlying the balance between cell-survival and cell-death signals initiated by UPR activation in cancers is unclear. The UPR serves to protect the cells from normal variations occurring in the cellular environment, which arise from changes in the blood nutrient levels and increase in toxic substances. A range of pathological conditions can also activate the UPR. Tumor cells encounter deficiency of oxygen and nutrients. Under such circumstances, the UPR can be induced in these cells. Furthermore, tumor cells produce several survival factors such as autocrine or paracrine stimulators, invasion and metastatic regulators such as matrix metalloproteinases, and transmembrane proteins such as adhesion molecules to initiate survival formation around the microenvironments. Several studies have indicated that UPR activation probably plays a crucial role in tumor growth. It has been demonstrated using XBP1-deficient cells and XBP1-knockdown cells that XBP1 is required for tumor growth in vivo [8]. The XBP1-induced UPR has also been shown to play a key role in the pathogenesis of plasma cell myeloma [9]. Our preliminary observation indicated that UPR was also upregulated in some primary Ph-negative leukemia cells (data not shown). Therefore, the activation of the UPR might be a common mechanism in both solid tumor and leukemia cells. We showed that the suppression of the UPR enhanced the anti-leukemic effects of imatinib and etoposide in Bcr-Abl-expressing cells. In Ph-positive leukemia cells, the apoptosis-inducing mechanism of imatinib was considerably different from that of etoposide. Therefore, targeting the UPR may provide useful alternative approaches for the treatment of Ph-positive leukemia such as an imatinib resistant-CML clone or Ph-positive acute leukemia.

Conflict of interest statement

The authors declare no competing financial interests.

Acknowledgements

This work was supported by Grants-in-Aid from the Ministry of Education, Culture, Sports, Science and Technology, Japan; UBE Kosan Foundation; and Yamaguchi University Foundation.

Contributions: All authors contributed to this paper; in particular, A.T., T.Y., Y.T., M.H., N.M., and Y.N. contributed to experimental work. T.Y. wrote the manuscript. K.M. and Y.T. contributed to the proofreading of the manuscript.

References

[1] Ma Y, Hendershot LM. The role of the unfolded protein response in tumour development: friend or foe? Nat Rev Cancer 2004;4:966–77.
[2] Miyoshi K, Katayama T, Imaizumi K, Taniguchi M, Mori Y, Hitomi J, et al. Characterization of mouse Ire1 alpha: cloning, mRNA localization in the brain and functional analysis in a neural cell line. Brain Res Mol: Brain Res 2000;85:68–76.
[3] Yoshida H, Okada T, Haze K, Yanagi H, Yura T, Negishi M, et al. ATF6 activated by proteolysis binds in the presence of NF-Y (CBF) directly to the cis-acting element responsible for the mammalian unfolded protein response. Mol Cell Biol 2000;20:6755–67.
[4] Yoshida H, Matsui T, Hosokawa N, Kaufman RJ, Nagata K, Mori K. A time-dependent phase shift in the mammalian unfolded protein response. Dev Cell 2003;4:265–71.
[5] Yamamoto K, Sato T, Matsui T, Sato M, Okada T, Yoshida H, et al. Transcriptional induction of mammalian ER quality control proteins is mediated by single or combined action of ATF6alpha and XBP1. Dev Cell 2007;13:365–76.
[6] Urano F, Wang X, Bertolotti A, Zhang Y, Chung P, Harding HP, et al. Coupling of stress in the ER to activation of JNK protein kinases by transmembrane protein kinase IRE1. Science 2000;287:664–6.
[7] Hetz C, Bernasconi P, Fisher J, Lee AH, Bassik MC, Antonsson B, et al. Proapoptotic BAX and BAK modulate the unfolded protein response by a direct interaction with IRE1alpha. Science 2006;312:572–6.
[8] Romero-Ramirez L, Cao H, Nelson D, Hammond E, Lee AH, Yoshida H, et al. XBP1 is essential for survival under hypoxic conditions and is required for tumor growth. Cancer Res 2004;64:5943–7.
[9] Carrasco DR, Sukhdeo K, Protopopova M, Sinha R, Enos M, Carrasco DE, et al. The differentiation and stress response factor XBP-1 drives multiple myeloma pathogenesis. Cancer Cell 2007;11:349–60.